NAVAL POSTGRADUATE SCHOOL
MONTEREY, CALIFORNIA

THESIS

PRELIMINARY VIBRATION SURVEY OF A SUSPENDED FULL-SCALE OH-6A HELICOPTER FROM 0 TO 45 HZ

by

John H. Harris, III

March, 1996

Thesis Advisor: E. Roberts Wood
Co-Advisor Joshua H. Gordis

Approved for public release; distribution is unlimited.

REPORT DOCUMENTATION PAGE

Form Approved OMB No. 0704-0188

1. AGENCY USE ONLY *(Leave blank)*	2. REPORT DATE March 1996	3. REPORT TYPE AND DATES COVERED Master's Thesis

4. TITLE AND SUBTITLE Preliminary Vibration Survey of a Suspended Full-Scale OH-6A Helicopter from 0 to 45 Hz

5. FUNDING NUMBERS

6. AUTHOR(S) Harris, John H., III

7. PERFORMING ORGANIZATION NAME(S) AND ADDRESS(ES)
Naval Postgraduate School
Monterey CA 93943-5000

8. PERFORMING ORGANIZATION REPORT NUMBER

9. SPONSORING/MONITORING AGENCY NAME(S) AND ADDRESS(ES)

10. SPONSORING/MONITORING AGENCY REPORT NUMBER

11. SUPPLEMENTARY NOTES The views expressed in this thesis are those of the author and do not reflect the official policy or position of the Department of Defense or the U.S. Government.

12a. DISTRIBUTION/AVAILABILITY STATEMENT
Approved for public release; distribution is unlimited.

12b. DISTRIBUTION CODE

13. ABSTRACT *(maximum 200 words)*

Efforts to establish a helicopter research program in structural dynamics at NPS were greatly enhanced when the U. S. Army donated two OH-6A light observation helicopters. One of the helicopters is reserved for ground vibration testing and dynamics research. Vibration measurements are extremely important in predicting and understanding an aircraft's dynamic behavior and durability. A comparison of a helicopter's natural frequencies and those frequencies transmitted to the airframe through the rotor system can alert the designer/evaluator to possible dynamic problems. This thesis establishes a baseline vibration test program on the OH-6A helicopter for future testing and comparison to analytic models. The goal of the research is to establish natural frequencies (eigenvalues), principal mode shapes (eigenvectors), and damping characteristics of the OH-6A and to compare these values to test and analytical data obtained from the McDonnell Douglas Helicopter Company.

14. SUBJECT TERMS Helicopter, Vibration Analysis, Vibration Testing, Natural Frequencies, Mode Shapes, Structural Damping, Vibration Forced Response, Structural Dynamics

15. NUMBER OF PAGES 75

16. PRICE CODE

17. SECURITY CLASSIFICATION OF REPORT	18. SECURITY CLASSIFICATION OF THIS PAGE	19. SECURITY CLASSIFICATION OF ABSTRACT	20. LIMITATION OF ABSTRACT
Unclassified	Unclassified	Unclassified	UL

NSN 7540-01-280-5500

Standard Form 298 (Rev. 2-89)
Prescribed by ANSI Std. 239-18 298-102

Approved for public release; distribution is unlimited.

PRELIMINARY VIBRATION SURVEY OF A SUSPENDED FULL-SCALE OH-6A HELICOPTER FROM 0 TO 45 HZ

John H. Harris, III
Lieutenant, United States Navy
B.S, Pennsylvania State University, 1988

Submitted in partial fulfillment
of the requirements for the degree of

MASTER OF SCIENCE IN AERONAUTICAL ENGINEERING

from the

NAVAL POSTGRADUATE SCHOOL
March 1996

ABSTRACT

Efforts to establish a helicopter research program in structural dynamics at NPS were greatly enhanced when the U. S. Army donated two OH-6A light observation helicopters. One of the helicopters is reserved for ground vibration testing and dynamics research. Vibration measurements are extremely important in predicting and understanding an aircraft's dynamic behavior and durability. A comparison of a helicopter's natural frequencies and those frequencies transmitted to the airframe through the rotor system can alert the designer/evaluator to possible dynamic problems. This thesis establishes a baseline vibration test program on the OH-6A helicopter for future testing and comparison to analytic models. The goal of the research is to establish natural frequencies (eigenvalues), principal mode shapes (eigenvectors), and damping characteristics of the OH-6A and to compare these values to test and analytical data obtained from the McDonnell Douglas Helicopter Company.

TABLE OF CONTENTS

ACKNOWLEDGEMENTS

Preparing for and performing a vibration test on a full-scale helicopter is not something that can be accomplished by an individual in the amount of time allotted for an NPS thesis. The author, therefore, relied on numerous individuals for guidance, support, and help throughout his thesis work, and would like to take this opportunity to thank them.

First and most importantly, I would like to thank my wife, Stephanie, and daughter, Abigail, for their continuous support and inspiration during our stay in Monterey and throughout my career in the U. S. Navy. Additionally, Dr. E. R. Wood devoted countless hours advising me through this often-times intimidating and complex subject. He is, without a doubt, one of the strongest proponents of the helicopter, and his enthusiasm for the subject is infectious. His vision for a rotorcraft dynamics research facility could prove to be one of the most important concepts proposed to NPS in quite a while. Dr. J. H. Gordis, through the Mechanical Engineering department, supplied the test equipment and the expertise required to perform the actual vibration test. Tom McCord, also from the M.E. department, was instrumental in providing a test facility and configuring equipment for the vibration test.

Special thanks go to the following for their time, effort, and interest: Dr. D. A. Danielson, Dr. E. M. Wu, Warrant Officer Tim Tompkins, John Molton, and LCDR James Speer.

Finally, I would like to thank the staff and faculty of NPS, especially the Aeronautical Engineering Department, for affording me the opportunity to study a field far removed from my undergraduate degree in Finance.

I. INTRODUCTION

A. GENERAL

Structural dynamics play an essential role in every facet of helicopter design and evaluation. Indeed, one of the greatest challenges that faces the rotorcraft industry today is vibration reduction. A solution to this problem requires a full understanding of helicopter vibration, namely, how the main and tail rotors act as a vibration source and the resulting airframe response.

The airframe response to vibratory excitations requires a thorough knowledge of natural frequencies, mode shapes, and structural damping. These characteristics are generally obtained in two ways, analytic modeling and vibration testing. Incidentally, testing serves as a verification for analytic models. Therefore, until the dynamicist can predict dynamic characteristics with unquestionable certainty, vibration testing will remain an essential tool to the helicopter community.

B. SCOPE

The purpose of this thesis was to launch a rotorcraft dynamics program at the Naval Post Graduate School (NPS) by conducting a preliminary vibration test on a McDonnell Douglas OH-6A light observation helicopter. The testing evaluated frequencies from 0 to 45 Hz. The primary goal of the research was to obtain natural frequencies, mode shapes, and damping characteristics of the principal modes within the above prescribed frequency range.

II. BACKGROUND

A. VIBRATION THEORY

The subject of vibration deals with the behavior of bodies under the influence of oscillatory forces. Such forces can be produced by unbalance in rotating machinery, or in the case of the helicopter by vibratory airloads acting on the main or tail rotor blades.

Vibrations fall into three general classes: free, forced, and self-excited. Free vibration occurs when an elastic system (such as a simple spring mass system) vibrates under the action of forces inherent in the system itself, and without external impressed forces. A system under free vibration will vibrate at one or more of its natural frequencies. Vibration that results from the excitation of external forces is called forced vibration. Here dynamic external forces are applied at frequencies independent of the natural frequencies of the system. When the frequency of the exciting force coincides with a natural frequency of the body, a condition known as resonance is encountered. Resonance is especially dangerous because large displacement amplitudes result, which, in turn, create large stresses and strains on the body. Self-excited vibration results in divergent oscillations where the system damping is negative.

Nearly all vibrating systems are subject to damping, which can be positive or negative. Positive damping causes the motion in free vibrating systems to decay, whereas forced vibration systems can be maintained at constant amplitude due to the energy supplied by the external force. In negatively damped systems, the damping force acts as a driving force and does positive work on the system. The work done by this force is converted into the additional kinetic energy of the increased vibration. Negative damping

requires an external source of energy. In the well-known case of flutter, the airflow itself provides this source of energy. [Ref.1]

Damping is often defined in terms of the damping ratio, ζ, which is the ratio of the damping coefficient to the critical damping coefficient, or c/c_c. For positive damping, three cases exist:

1. $\zeta < 1$, Underdamped motion results in the system decaying in an oscillatory manner
2. $\zeta > 1$, Overdamped motion results in the system decaying in a non-oscillatory manner,
3. $\zeta = 1$, Critically damped motion separates oscillatory decay from non-oscillatory decay.

The number of coordinates required to explain the motion of a system defines the degrees of freedom. A simple pendulum, for example, has one degree of freedom, whereas a stretched string, a vibrating beam, or any continuous system vibrates with infinite degrees of freedom. Systems with many degrees of freedom can vibrate in a complex manner. They can be treated mathematically by the superposition of their individual dynamic patterns called principal "normal" modes. The term "normal mode" comes from the fact that the individual modes can be shown in a vector sense to be normal or at right angles to each other. Mathematically this is known as the property of orthogonality. A system with *n* principal modes has *n* natural frequencies. In many cases, the lowest natural frequencies (fundamental frequencies) of the system are the most important.

1. Forced Vibration

Applications in this thesis deal with forced vibrations. A system under the action of a harmonic force such as $F = F_0 \sin \omega t$ assumes an equation of motion in the form:

$$m\ddot{x} + c\dot{x} + kx = F_0 \sin\omega t \tag{1}$$

which can also be expressed as the vector relation:

$$\textit{Inertia force} + \textit{damping force} + \textit{spring force} + \textit{impressed force} = 0 \tag{2}$$

The steady-state oscillation that remains after the transient motion disappears may be expressed as:

$$x = X \sin(\omega t - \Phi) \tag{3}$$

where X is the amplitude of steady oscillation and Φ is the phase angle by which the motion of the system lags the impressed force. Substituting the above solution into the original differential equation, the following vector relation results:

$$m\omega^2 X \sin(\omega t - \Phi) - c\omega X \sin(\omega t - \Phi + \Pi/2) - kX \sin(\omega t - \Phi) + F_0 \sin \omega t = 0 \tag{4}$$

This vector relation can be shown graphically as in Figure 1. The complete solution to Eqn. 1 is given by the following equation:

$$x = X_1 e^{-\zeta \omega_n t} \sin\left(\sqrt{1-\zeta^2}\ \omega_n t + \phi_1\right) + \frac{F_0 \sin(\omega t - \phi)}{\sqrt{(k - m\omega^2)^2 + (c\omega)^2}} \tag{5}$$

or

$$x = x_{transient} + x_{steady\ state.}$$

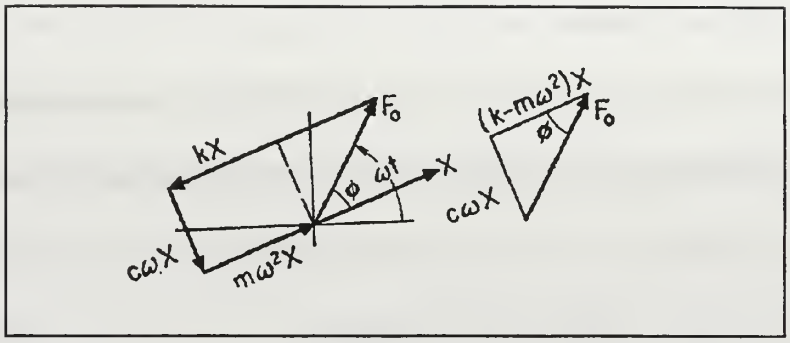

Figure 1. Vector Representation of Forced Vibration With Viscous Damping. From [Ref. 2].

Here, the transient solution is also known as the complementary solution, and the steady state solution can be referred to as the particular solution. The expressions above can be reduced in terms of the following quantities: [Ref 2]

$\omega_n = \sqrt{(k/m)}$ natural frequency of undamped oscillation

$\zeta = c/c_c$ damping factor

$c_c = 2m\omega_n$ critical damping coefficient

$$X = \frac{F_0}{\sqrt{(k - m\omega^2)^2 + (c\omega)^2}}$$ amplitude of steady oscillation

$$\tan \phi = \frac{c\omega}{k - m\omega^2}$$ phase angle by which motion lags impressed force.

$$\frac{X}{X_0} = \frac{1}{\sqrt{[1 - (\frac{\omega}{\omega_n})^2]^2 + (2\zeta\frac{\omega}{\omega_n})^2}}$$ magnification factor (nondimensionalized)

$$\tan \phi = \frac{2\zeta \frac{\omega}{\omega_n}}{1 - (\frac{\omega}{\omega_n})^2} \qquad \text{nondimensionalized } \phi$$

At steady-state resonance, ω is equal to ω_n, the phase angle, ϕ, is 90 degrees, and the amplitude, X, becomes $F_0/c\omega_n$. For small values of $\omega/\omega_n << 1.0$ the phase angle remains small (zero for undamped systems), while at large values of $\omega/\omega_n >> 1.0$ the phase angle approaches 180 degrees (exactly 180 degrees for an undamped system). Therefore, a 180 degree phase shift occurs as resonance is passed. In a multi-degree of freedom system, a 180 degree phase shift occurs each time a resonant frequency is passed. This important phenomenon aids in detecting resonance. Steady-state resonance also implies that the inertia force and spring force cancel each other, while the damping force cancels the impressed force. If the damping force is plotted on the imaginary axis, and inertial and spring forces are plotted on the real axis, then the imaginary values encounter a peak when resonance occurs. Likewise, the real values pass through zero during resonance.

B. HELICOPTER VIBRATIONS

Helicopters are inherently vibratory machines due to their rotating components which produce lift and thrust. However, the elimination, reduction, and avoidance of vibration are important to helicopter operations for the following reasons:

1. to provide comfort for the crew and passengers, and

2. to minimize fatigue to the airframe and components.

It is therefore essential that vibration analysis be an integral part of helicopter design and testing.

Vibrations are mainly caused by periodic aerodynamic loads transferred from the main rotor to the fuselage via the hub. The tail rotor also generates vibrations in a similar manner. Other sources of vibration include engines, transmissions, and aerodynamic forces on the fuselage.

An abiding goal of helicopter design has been to decrease fuselage vibrations to levels that are consistent with fixed wing aircraft. This "jet-smooth" ride is defined as approximately 0.02 g's. Presently, the reduction of vibrations to this level remains elusive. Figure 2 shows that while a significant reduction in vibration has been achieved by industry in the twenty-five years considered, it also illustrates an asymptotic trend at 0.10 g. Therefore, quantum advances in vibration control technology are required to reach the goal of 0.02 g. [Ref 3]

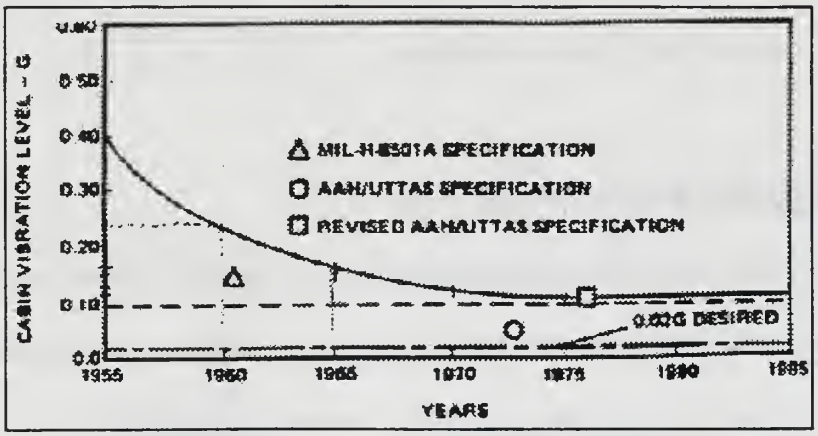

Figure 2. Trend of Helicopter Vibration Levels Since 1955. From [Ref. 3].

The two principal difficulties intrinsic to solving the helicopter vibration dilemma are:

1. obtaining precise knowledge of the loads acting on the rotor and airframe, and
2. calculating accurate airframe dynamic characteristics such as natural frequencies, mode shapes, and damping factors.

Historically, passive techniques were employed in combating the vibration problem. Such methods included the installation of isolation mounts and vibration absorbers and the application of damping materials. Currently, research is being conducted in attempts to actively reduce vibrations. These methods attack the problem at its source, the rotor. Higher Harmonic Control (HHC) and Individual Blade Control (IBC) are two such active reduction methods. Both methods suppress vibration with inputs to the main rotor which alter the aerodynamic loads on the rotor blades such that the blade response and resulting blade root shears are reduced. [Ref. 3]

Regardless of the vibration suppression method employed, knowledge of the structural dynamic characteristics of the helicopter is paramount in keeping vibrations to a minimum. Most often, this knowledge is gained through computer aided modeling of the structure which is supported with vibration tests of the actual structure.

1. Exciting Forces

Helicopter vibrations generally fall into three categories. These are: 1) vibrations due to rotor excitation which are at integral multiples of the rotor's rotational speed; 2) vibration due to random aerodynamic excitation where the observed frequency is a natural

frequency of the airframe structure; and 3) self-excited vibrations, such as flutter and ground resonance. [Ref 1]

a. Vibrations at Integral Multiples of Rotor Speed

Most helicopter vibrations emanate from the main and tail rotors where harmonics of aerodynamic loads on the blade give rise to the vibratory response of the blade. Since the blade is attached to the hub at the root, the blade responses result in root shears which feed from the rotor head into the fuselage as vibratory shears and moments . The rotor system acts as a filter in passing these forces into the airframe. The frequencies of concern are typically integer multiples of *n/rev* (*nP*) harmonics, where *n* is the number of rotor blades. Experience has shown that the *nP,* or blade passage frequency, is the most critical. For example, a four-bladed helicopter's critical frequency is *4P*. [Ref 1]

For an *n-bladed* helicopter, the *nP* airframe vibrations result from the higher harmonic blade airloads. The sources of this loading are the rotor wake and stall and compressibility effects. Figure 3 shows that in a hover, these effects are relatively small due to the small aerodynamic asymmetries involved. However in transition from hover to forward flight, the *nP* vibrations increase dramatically due to wake-induced loads on the rotor. Here the wake of the rotor remains close to the plane of the disk. Similar phenomena occur during deceleration and descent. In these transition cases, the blades interact with the vortices of preceding blades (blade-vortex interaction or BVI), producing higher harmonic airloading, which can be transmitted to the airframe. As speed increases, the wake of the rotor is pushed away from the disk plane and vibration decreases, as

shown in the 80 knot regime of Figure 3. At high speeds vibration reappears due to retreating blade stall and advancing blade compressibility, which again produce higher harmonic loading.

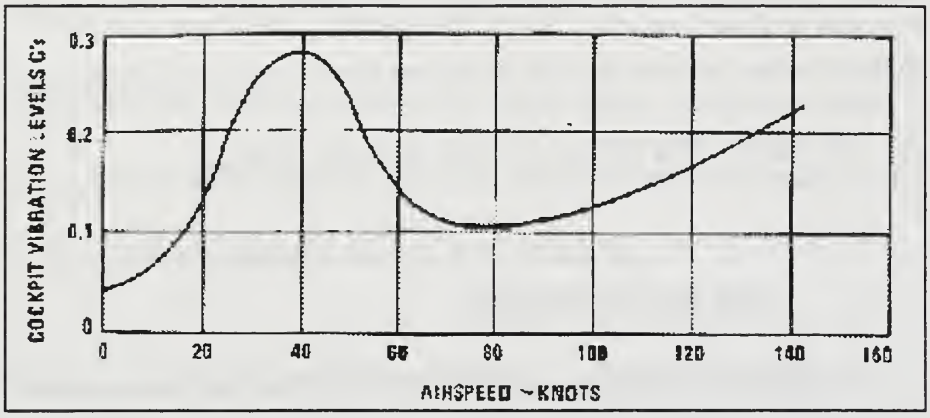

Figure 3. Helicopter Vibration Variation with Airspeed. From [Ref. 1].

Other excitation frequencies also emanate from the rotor system. One of the most prevalent frequencies transferred to the fuselage is the *1/rev* (*1P*), which results from any aerodynamic or inertial unbalance in the rotor blades. Additionally, any unbalance of blade dampers may cause *2/rev* (*2P*) excitation. Therefore, much effort is placed on balancing and tracking rotors and matching blade damper characteristics to reduce these differences. The inertial properties of the blades can be tuned by attaching small weights, while the aerodynamic properties can be equalized by adjusting trim tabs or pitch links.

b. Vibrations Due to Random Aerodynamic Excitation

In forward flight, turbulent downwash from the main rotor can impinge on the fuselage and the horizontal tail. This excitation has been found to be rich in harmonics which can create vibration problems by exciting fundamental aircraft or empennage modes. Solutions to this problem include modifying the structure and altering the flow from the rotor hub region using fairings or other methods. [Ref 1]

c. Self-Excited Vibrations

In self-excited vibration, divergent oscillations occur due to negative system damping, as discussed previously. Here the damping force acts as a driving force and performs positive work on the system. This work is converted into additional kinetic energy of the increased vibration. Self-excited vibration cannot exist without an external source of energy. Two well-known sources of external energy for this phenomena include flutter and ground resonance. [Ref 1]

2. The Rotor as a Filter

Every rotor system (articulated, rigid, teetering, etc.) incorporates into the rotor hub design some method of relieving the flapping and lead-lag bending moments at the blade root. However, flapping and lead-lag shear forces still exist at the blade-hub attachment point. These forces sum at the hub and then transmit to the fuselage. Gerstenberger and Wood [Ref. 4] provide an excellent discussion showing that for an n-bladed rotor system, only the nP harmonics will be seen in the fixed system. All other

forces exactly cancel at the hub, assuming all blades are perfectly balanced, steady-state flight, and each blade has the same time history as its neighboring blades. In effect, the rotor acts as a filter. Table 1 lists the forces and moments present in the rotating system and the resulting frequencies of the forces and moments that feed into the non-rotating airframe. Note that p represents an integer multiplier. The end result is that nP and $1P$ harmonics dominate the vibration produced by actual rotors. Keeping in mind that the helicopter is a constant RPM machine, vibration reduction becomes easier, in general, since only a few known frequencies need to be considered.

Rotating Frame (Rotor)	Non-Rotating Frame (Fuselage)
vertical shear at pN/rev	thrust at pN/rev
lagwise moment at pN/rev	torque at pN/rev
in-plane shear at pN ± 1/rev	rotor drag and side forces at pN/rev
flapwise moment at pN ± 1/rev	pitch and roll moments at pN/rev
feathering moments at pN/rev	collective control system forces at pN/ rev
feathering moments at pN ± 1/rev	cyclic control system forces at pN/rev

Table 1. Transmission of Vibration Through the Rotor Hub. From [Ref. 5].

3. The Fuselage Response

The vibration at a particular point of the helicopter is due to the fuselage response to the aforementioned exciting forces. A basic principle in designing an airframe which minimizes vibration is to avoid proximity to structural resonances which may be excited by

rotor-transferred frequencies, particularly the *1P* and *nP* harmonics. Therefore, vibration design of the helicopter requires an accurate prediction and verification of the resonant frequencies and mode shapes of the fuselage prior to development of the prototype aircraft and full-scale production. Mode shapes are important because they show where the points of highest amplitude occur.

Prediction of fuselage resonant frequencies and mode shapes is a very complicated problem due to the intricate nature of the structure involved. Today finite element methods are used for these calculations. This process regards the fuselage as an assembly of elements possessing certain mass and stiffness. Straightforward but lengthy calculations are then performed using a computer. NASTRAN, PATRAN, and I-DEAS are popular finite element programs for these computations. Once correlated with vibration tests of the full-scale helicopter, these same finite element programs can be used to research changes in the design should problems be encountered during flight test development of the new helicopter.

C. HUGHES OH-6A HELICOPTER

1. Acquisition

Two OH-6A helicopters arrived at NPS in October, 1995. This event was the culmination of more than a year's work needed to ensure a smooth transfer of ownership from the U. S. Army to NPS. Many individuals were responsible for obtaining the helicopters. Through the persistent efforts of LTG William Forster, USA (Retired), Dr. E. Roberts Wood, and MAJ Derle G. Hagwood, USMC, a military directive was issued

which authorized the shipment of two flightworthy helicopters from Westover Air Force Base, Massachusetts to the Naval Post Graduate School.

The logistics of moving the aircraft from Massachusetts to Monterey proved to be a difficult task. CW2 Tim Tompkins and LTCOL Dan Nichols from the Army National guard at Westover Air Force Base served as liaisons between NPS and the Army. The author worked with them in planning the details of the transportation. The two helicopters were carried by a C-5A Galaxy to Travis Air Force Base. The Public Works department of NPS conducted the final leg of the trip by transporting the helicopters on a flatbed truck from Travis Air Force Base to Monterey.

2. OH-6A Characteristics and Background

The OH-6A aircraft (Figure 4) is a four place, dual piloted, single engine observation helicopter manufactured by McDonnell Douglas Helicopter Corporation (formerly Hughes Helicopter) . It is equipped with a single four-bladed main rotor, a two-bladed tail rotor, and an oleo-damped skid-type landing gear. A unique feature of the helicopter is that it incorporates a static mast concept, through which flight loads are transmitted directly into the airframe, and not through the main transmission. This feature was incorporated into the U. S. Army's AH-64 "Apache" attack helicopter and more recently into the Boeing-Sikorsky RAH-66 "Comanche" helicopter.

The main rotor incorporates an articulated system with lead-lag, flapping, and feathering hinges. Rotation of the main rotor is 483 RPM at 100% Nr. Therefore the *1P* frequency is approximately 8 Hz, and the *4P* is approximately 32 Hz.

Figure 4. NPS Dynamics Research OH-6A Light Observation Helicopter

The U.S. Army, and later, Army National Guard units, used the OH-6A's throughout the 1960's, 1970's and 1980's and is currently phasing them out along with the OH-58 Kiowa's. The aircraft built a strong reputation during its service life, providing service dating from Vietnam to Desert Storm. Two of the OH-6A's greatest assets were its crashworthiness and extremely low drag. Many stories have surfaced that describe the egg-shaped airframe acting as a protective shell when the aircraft impacted the ground due to enemy ground fire, thus preventing serious injury to the crew.

3. NPS Plans for the OH-6A's

Present plans for the NPS OH-6A's are twofold. According to Dr. Wood, one aircraft will remain operational, and will be based at the Marina airport in support of the flight test center currently being organized by CAPT(Ret) Tom Hoivik, USN of the Operations Research department at NPS. The second helicopter will continue to serve as a dynamics laboratory research tool. Recently, requests have been made for vibration test equipment for the aeronautical engineering department at NPS. If approved, the laboratory helicopter would serve as an excellent hands-on vibration analysis demonstration or experiment. The main rotor hub and blades of the laboratory aircraft are scheduled to be used for HHC performance testing as part of the SatCon Technology Corporation SBIR with the Naval Air Weapons Center (NAWC).

4. Structural Characteristics of the OH-6A

The OH-6A airframe is a very durable structure known for its crash survivability. The airframe is composed of the fuselage, tailboom, and empennage, which include primary and secondary structure consisting of all metal, metal and fiberglass, and transparent plastic components. The principle structural member of the aircraft is the reinforced floor center section, which consists of a riveted and bolted assembly of aluminum alloy frames, stiffeners and doublers. The Department of the Army [Ref. 6] states that the basic body and tailboom are conventional, metal, riveted structures incorporating formed aluminum alloy, stainless steel and titanium bulkheads, canted frames, channel members, beams, structure rings, ribs, stiffeners, doublers, longerons, and

stringers. All stressed skin panels are either smooth or beaded and the stabilizers are all-metal airfoils. The tailboom is a conventional semi-monocoque structure consisting of a frame comprised of stringers and bulkheads with sheet metal outer skin.

Aircraft stations are assigned by determining the respective longitudinal distances aft of the most forward part of the structure (i.e., the forward edge of the main rotor disk). Therefore, the fuselage, tailboom, and empennage stations range from 28.00 to 290.00 as depicted in Figure 5.

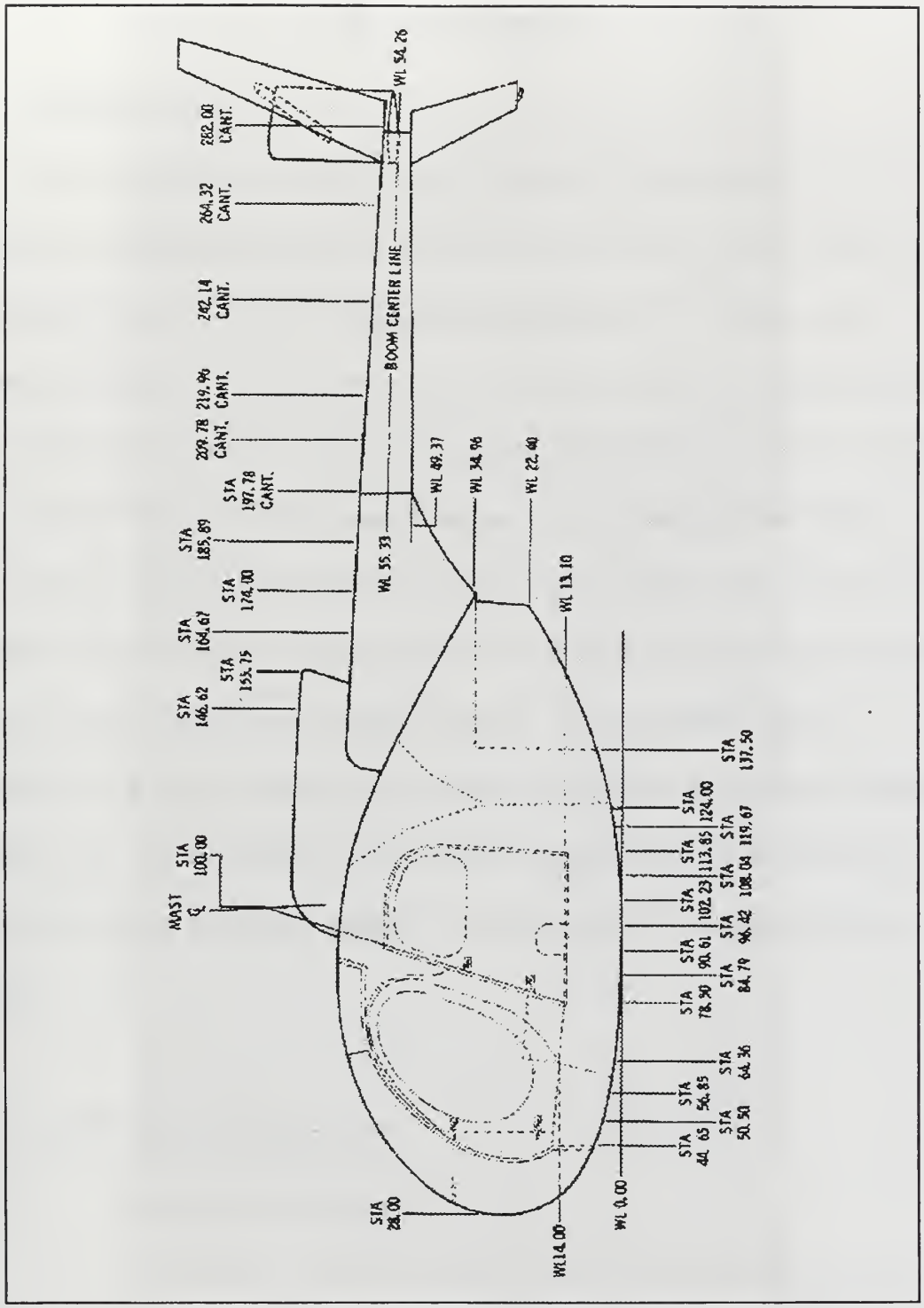

Figure 5. OH-6A Fuselage Stations. From [Ref.6].

III. RESEARCH

A. OVERVIEW

The proposed thesis research involved conducting a vibration test on an OH-6A airframe and comparing the results to prior vibration tests as well as results obtained from a previously constructed NASTRAN finite element model [Ref. 7]. Shake testing identified the fuselage natural frequencies and mode shapes of primary interest, especially those adjacent to multiples of blade passage frequencies, specifically *1P* and *4P*. The goal was to determine the main modes, natural frequencies, and damping of the OH-6A structure and to hopefully corroborate the three sources of OH-6A data. The test was intended to identify the primary modes from 0 to 45 Hz. and to serve as a baseline test for further vibration experiments and dynamic analyses. The experimental methods incorporated in the thesis were purposely designed to provide an accurate and preliminary vibration survey in a timely fashion, while using a minimal amount of test equipment. More complex and sophisticated methods of vibration testing are planned for future research.

B. TEST PREPARATIONS

1. The Suspension System

The first requirement in performing ground-based helicopter vibration tests is to provide the aircraft with low frequency isolation (less than 1 Hz.) from outside interference, thereby ensuring a flight-like testing environment. Two primary methods are

typically used. The first involves placing the aircraft on an air cushion using devices such as airbags or airsprings. The second entails suspending the aircraft using shock absorber cord such as bungee. For helicopters, the preferred method is to suspend the helicopter from the main rotor hub as in Figure 6. Among aircraft so tested are the H-3, S-76, AH-64, RAH-66, and others.

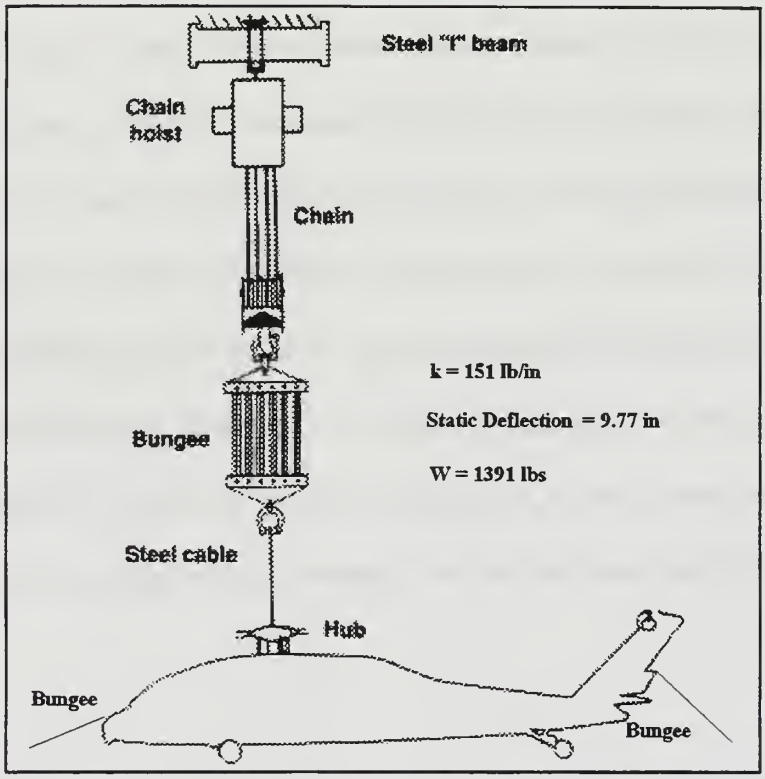

Figure 6. Typical Helicopter Vibration Suspension System Modified for OH-6A Parameters. From [Ref. 8].

The suspension system had several requirements. First, the natural frequency of the suspension was required to be low enough to avoid interfering with the natural frequencies of the vibrating fuselage. A target frequency of 1 Hz (2π rad/sec) was

established. Assuming a weight, W, of 1475 lbs., the target spring stiffness, k, was then determined as follows:

$$m = W/g = 1475 / 386 = 3.82 \text{ lb-sec}^2/\text{in}, \quad (6)$$

$$k = m\omega^2 = (3.82) \cdot (2\Pi)^2 = 151 \text{ lb/in}. \quad (7)$$

W and the above calculated k, yielded a target elongation

$$\Delta l = W/k = 9.77 \text{ in}. \quad (8)$$

The next task involved finding the appropriate shock absorber cord which would produce the correct elongation and frequency characteristics. Military Specification C-5651B, reproduced in Table 2, provided elongation versus load information for various diameter shock absorber cord.

Cord Diameter	1/2"	5/8"	3/4"
50 % Elongation	80-120 lbs	100-180 lbs	200-350 lbs
75% Elongation	110-190 lbs	160-250 lbs	300-450 lbs
100 % Elongation	175-250 lbs	250-350 lbs	400-650 lbs
Breaking Strength	400 lbs	500 lbs	1000 lbs

Table 2. Physical Properties of Shock Absorber Cord. (Mil-Spec C-5651B).

Two factors determined the diameter of the cord that was ultimately chosen. First, 50% elongation was desired since the cord deteriorates more rapidly at greater elongations. Second, a block and tackle was the preferred method of integrating the cord into the suspension system because it allowed for easy adjustments. However, a block and tackle assembly limited the number of strands of cord used to distribute the load. The

largest reasonably priced pulleys available contained three sheaths. Thus, the load could be equally divided among seven strands of cord. The three-quarter inch diameter cord was the only one which could satisfy the above considerations.

The final version of the suspension system consisted of two main components, 1) a manual hoist rated at 3000 lbs, and 2) the above mentioned block and tackle assembly (Figure 7). The block and tackle included two, three sheath pulleys, and three-quarter

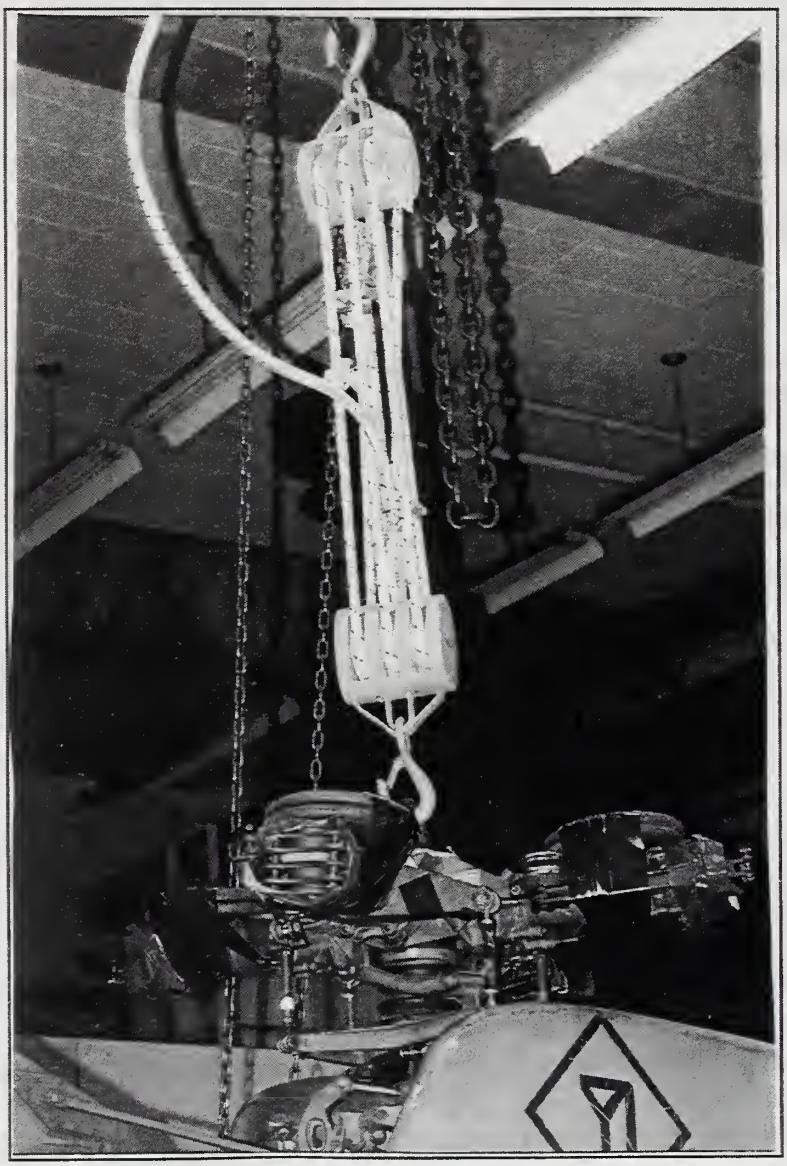

Figure 7. Helicopter Suspension System.

inch diameter bungee cord. The bungee cord was thereby mounted in a parallel spring arrangement comprised of seven cords (including the lead strand). The system distributed the load to approximately 210 pounds per strand. Trial and error adjustments to the initial length of the block and tackle assembly eventually produced the desired loaded elongation of approximately 10 inches.

The resulting natural frequency was verified by applying a vertical impulse to the main rotor hub, counting the subsequent number of oscillations during a ten-second period, and converting the results to cycles per second. By this method, the natural frequency of the system was found to be to be 0.9 Hz, which met the design goal of less than 1 Hz.

2. The Excitation Source Mount

The next required task involved selecting the input location of the harmonic excitation force. Criteria for the force input location included:

1. a hard point or primary structure,
2. an effective location for exciting structural modal characteristics (i.e., avoid node points), and
3. easy accessibility.

The lower cable cutter of the wire strike protection system (WSPS) on the OH-6A met these criteria. Located under the nose of the airframe, the cutter assembly attaches directly to the center beam (the main structural element of the fuselage) and provides easy access for the input force.

A mount was designed and manufactured to attach directly to the lower cable cutter. The design allowed for easy installation while maintaining the structural integrity of the airframe. Four bolts were removed from the cable cutter assembly, and their respective holes were used to position the mount. The mount design allowed for vertical, lateral, and a combination of vertical and lateral excitation. A clevis / rodend bearing assembly was also designed to ensure a moment-free application of the exciting force.

The final part needed to link the shaker to the aircraft was a drive rod or *stinger*. The stinger was made by tapering the middle section of a 12 inch brass rod with a 10/32 inch diameter. The rod proved to be flexible enough to prevent introducing moments into the system, and therefore, alleviated the requirement for the clevis / rodend bearing. The entire shaker assembly, including the excitation mount, load cell, stinger, and shaker, is shown in Figure 8.

3. Effective Blade Mass

To ensure proper free-flying qualities were reproduced in the shake-test aircraft, the mass of the main rotor blades had to be properly considered. The structure to be shake tested should be equivalent to 100% of the weight of all the actual aircraft items excluding the blades. The equivalent blade weight to be attached to the hub was reduced to 60% of the actual blade weight. [Ref. 8]. This supplied the fuselage with a rotor impedance closer to that provided to a free-flying aircraft with rotating flexible blades. Each rotor blade weighed 33.5 pounds, therefore, 20 pounds of weight were attached to each blade mounting point on the hub for a total of 80 pounds.

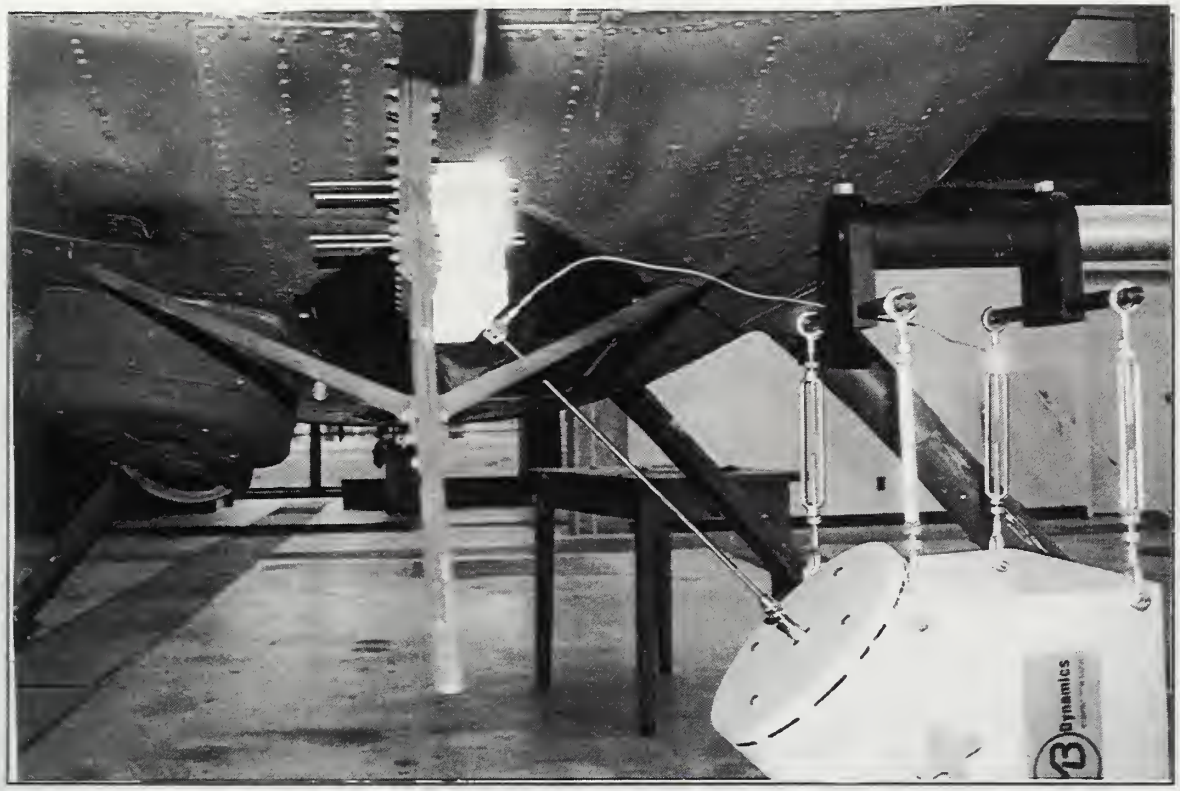

Figure 8. Shaker Assembly (Excitation Mount, Load Cell, Stinger, and Shaker).

4. Test Equipment

The basic layout of the test equipment is shown in Fig. 9. The principal apparatus is the Hewlett-Packard HP3562A Dynamic Signal Analyzer shown in Figure 10. The analyzer controls all facets of the test procedure. A source signal is generated by the analyzer, routed through a power amplifier, and sent to the MB Dynamics 50 lb. shaker. The load cell produces a signal corresponding to the load impressed on the aircraft by the shaker. This signal is sent through a signal conditioner and back to the analyzer via the input channel (channel 1). A roving accelerometer is attached to various aircraft points where it senses the acceleration resulting from the input load. The resulting signal is sent

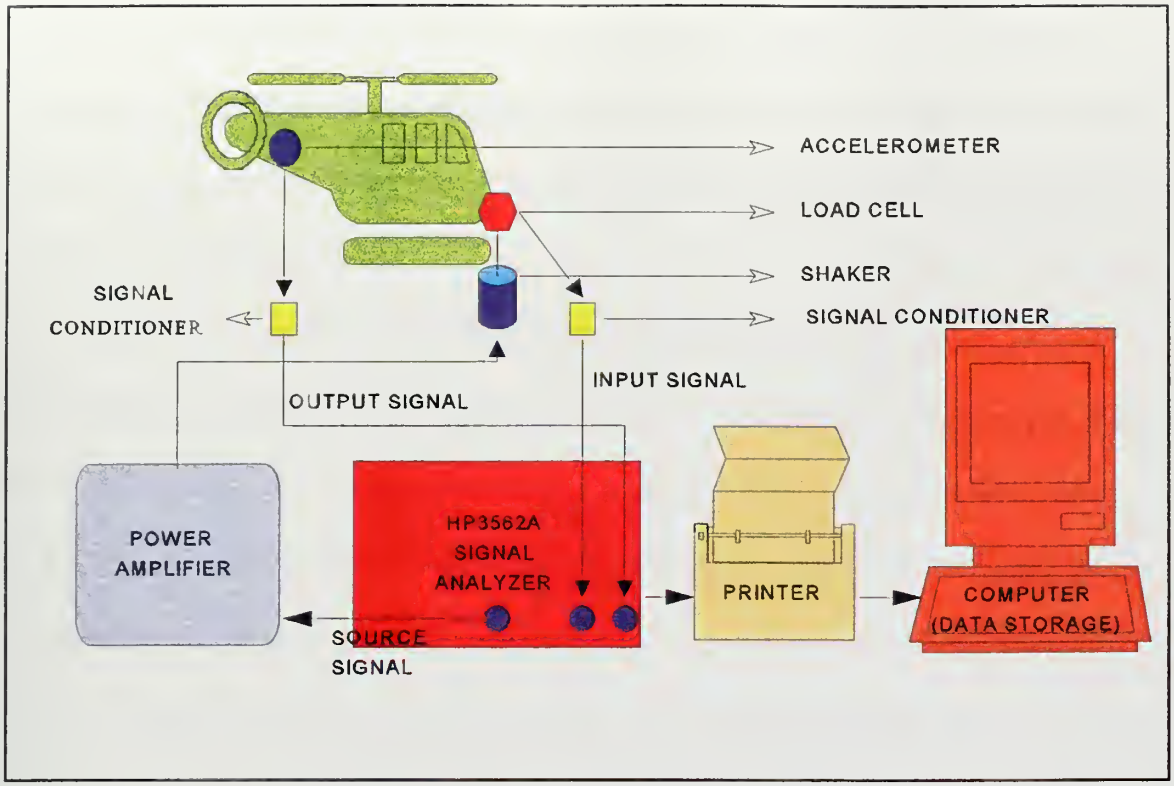

Figure 9. Vibration Test Configuration.

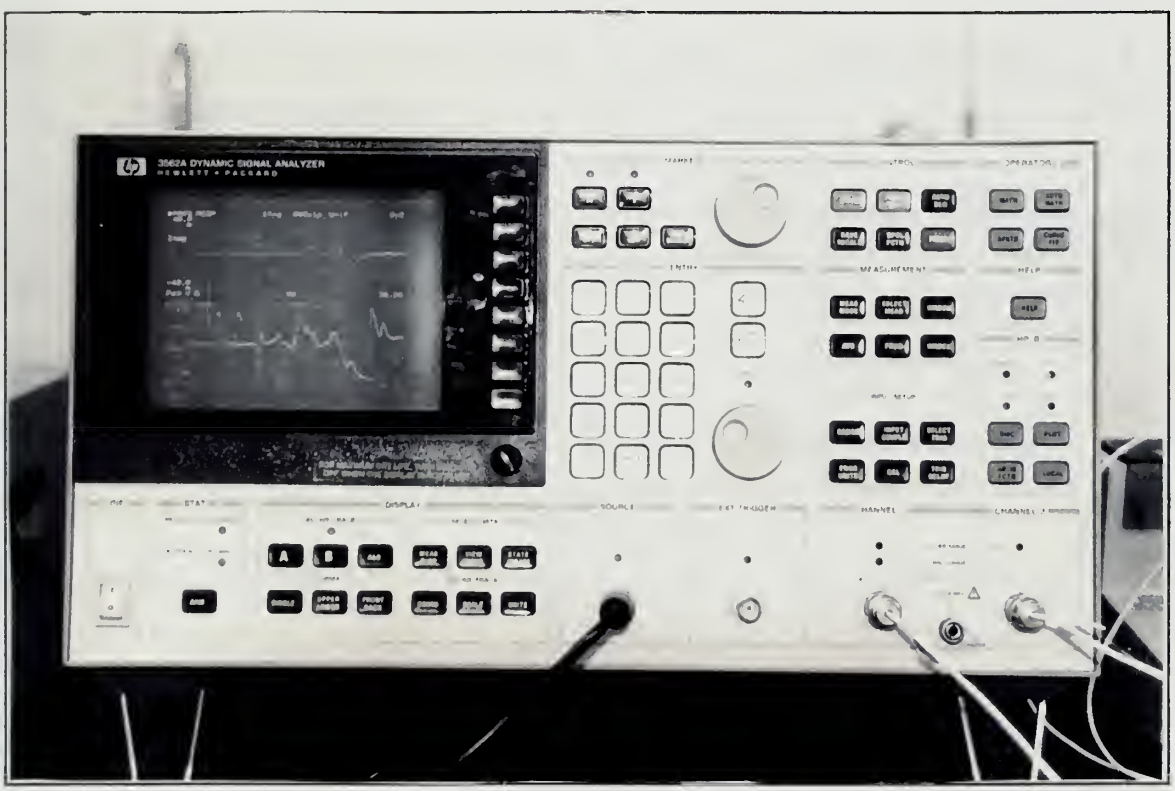

Figure 10. Hewlett-Packard HP 3562A Dynamic Signal Analyzer

through another signal conditioner and into the analyzer through the output channel (channel 2). Frequency response function (FRF) data is sent to the computer for storage and hard copies of the FRF are printed on the HP printer. and hard copies of the FRF are printed on the HP printer.

The primary method for exciting the helicopter airframe is with the use of an electromagnetic actuator configured as a 50 lb. shaker. This shaker has a dedicated power supply which is driven by a controlled vibratory voltage signal. A blower is attached to the shaker to provide cooling for high load / high frequency conditions. The shaker is connected to the airframe with two components:

1. a load cell which is attached directly to the excitation mount, and
2. the drive rod or *stinger*, which is threaded into the load cell.

The two basic measurement devices are the load cell and the accelerometer. The load cell is a piezoelectric device that deflects in response to an applied or inertial load. It is connected directly to the excitation mount, and provides the input signal for the analyzer. The accelerometer operates on the same principals as the load cell, however, the piezoelectric device deflects in response to acceleration vice load. The accelerometer is designed for maximum signal response due to accelerations along its vertical axis, although it also detects off-axis accelerations. Beeswax or chewing gum are used to mount the accelerometer directly on the airframe.

The HP 3562A Dynamic Signal Analyzer accepts two channels of analog data, and converts the signal using analog to digital conversion (A/D). Sampling rates can reach as high as several hundred kilohertz. A microprocessor is incorporated for dedicated

calculation of specific digital signal processing. A fast Fourier transform (FFT) algorithm forms the heart of the analysis and processing capabilities of the analyzer. The analyzer is capable of producing several specialized excitation signals for driving the shaker. Thus, straightforward signals such as a sweep of stationary harmonic frequencies with fixed increments can be produced, as well as a variety of nonstationary excitations such as burst chirps.

The main task accomplished by the analyzer is the calculation of a transfer function or frequency response function. This shows the mathematical measure of the linearity of channel B (output) to channel A (input). Noise can be a problem in obtaining accurate results, however, maximum utilization of averaging techniques allows the analyzer to filter out noise, thus enhance accuracy. Noise often occurs when force levels are low relative to background noise. A good measure of the reliability of test results is the coherence function, which provides a gauge for the linearity of the measured response [Ref. 8]. The nearness of the coherence measurement to unity indicates the degree to which the response at the accelerometer is linear to the input measured at the load cell. Near resonance, coherence values approach unity since the signals generated by the vibrating system are large and therefore less affected by noise [Ref.9].

The analyzer provides several testing modes including fixed frequency excitation, random excitation, frequency sweep excitation, and burst chirp and burst random excitation. Those modes primarily used in this analysis were the burst chirp and frequency sweep excitations. The burst chirp excitation supplies a signal during a specified percentage of the time record. Usually there is no signal at the start and end of the record.

The frequency sweep excitation entails continually increasing the frequency of excitation at a constant rate. Sweep rates can be manually increased or decreased.

The power spectrum function on the analyzer enables the user to determine input loads from the shaker. If the load cell sensitivity value is entered for the engineering units of channel one, the power spectrum function provides a direct readout of load as measured from the load cell. Similarly, acceleration values can be directly obtained from channel two.

Data storage is available with the use of any PC equipped with an IEEE 488.2 data acquisition card. A simple MATLAB program (see Appendix A) converts the data into the desired FRF output. Unfortunately, due to time constraints and hardware problems, data storage was not available for this thesis. However, storage remains an important tool for analyzing results and therefore warrants mention.

C. TEST PROCEDURE / RESULTS

1. Natural Frequency Determination

The first priority in the testing phase was to locate the natural frequencies between 0 and 45 Hz. Special attention was given to those frequencies in the vicinity of 8 Hz, *1P*, and 32 Hz, *4P*, since they are the most prevalent frequencies encountered in flight. The shaker / stinger was oriented at 45 degrees to excite vertical, lateral, and torsional modes simultaneously. A chirp burst from 1 to 45 Hz was initially performed to indicate the airframe natural frequencies of interest. Next, a series of three sine sweeps covering 1 to 17 Hz, 13 to 32 Hz and 28 to 48 Hz was input via the shaker and measured at three

discreet locations along the tail boom. This aided in further defining the natural frequencies of interest. Appendix B shows those frequency response functions with the most well-defined natural frequencies.

The following four criteria were used to determine the resonant frequency:

1. Imaginary scale spikes,
2. Real scale zero values,
3. Magnitude scale peaks, and
4. Phase scale phi (Φ) values of 90°.

The four criteria usually correlated within 0.05 Hz, except when two resonant frequencies were closely coupled within 1 Hz of each other. This resulted in some interference among the first three criteria. Hence, judgement had to be exercised in establishing the final resonant frequency value.

The modes were labeled according to the principal motion they produced, the number of nodes present, and their similarity to classical free-free beam modes. The region of highest response was typically most evident in the tailboom area, except when measurements were taken near a node. Table 3 provides a summary of modes and their respective natural frequencies.

2. Linearity of Resonant Frequencies

The next task involved determining the linearity of the resonant frequency response with varying load. The first lateral mode was chosen for this analysis because of its well-defined and easily observed reaction. A frequency sweep form 7 to 17 Hz was performed with the accelerometer mounted near the tail of the aircraft (station 274). A forced

Mode	Frequency (Hz)
1st Lateral	9.32
1st Vertical	9.97
1st Torsional	15.01
Aft Vertical	15.61
2nd Vertical	21.83
2nd Lateral	27.48
(Unnamed)	44.84

Table 3. Modal Natural Frequencies.

response was obtained for four different power settings ranging from 3.7 lbs to 38.0 lbs. The results, listed in Table 4, predict a nearly constant resonant frequency throughout the range of acceptable shaker input loads. The largest change in frequency was only 0.21%.

Force (lbs)	1st Lateral Freq (Hz)	1st Vertical Freq (Hz)
3.68	9.32	10.00
17.87	9.33	9.99
28.36	9.34	9.99
37.96	9.34	10.00

Table 4. Linearity of Resonant Frequencies.

3. First and Second Lateral Modes

Mode shapes were developed by measuring frequency response functions at various stations along the airframe. To excite the first and second lateral modes, the

shaker was attached to the airframe through the 45 degree attachment point (see Figure 9) of the excitation mount and a load of 17 lbs was applied. The accelerometer was mounted such that its vertical axis was horizontal to the floor and perpendicular to the longitudinal axis of the helicopter. This ensured maximum lateral pickup. The stations from which data was obtained are listed in Table 5. Note that the lateral mode measurement points were located along the port side of the aircraft, while the vertical mode measurement points were located along the top of the tailboom and the underside of the fuselage.

Point	Station (in.)	Point	Station
1	44.65	10	174.00
2	64.36	11	185.89
3	84.79	12	197.78
4	96.42	13	209.78
5	113.85	14	219.96
6	137.50	15	242.14
7	146.62	16	264.32
8	155.75	17	274.00
9	164.67		

Table 5. Accelerometer Measurement Points.

A plot of the imaginary values of the frequency response function revealed peaks and valleys at the resonant frequencies, while the real values approached zero. Since displacement was directly proportional to acceleration, the imaginary FRF values at the

peaks and valleys could be transformed into a modal curve by obtaining a value at each station along the airframe. Appendix C contains the MATLAB program used to plot the modal curve shown in Figure 11, as well as the remaining modal curves. The curve fit was accomplished using a fifth-order polynomial.

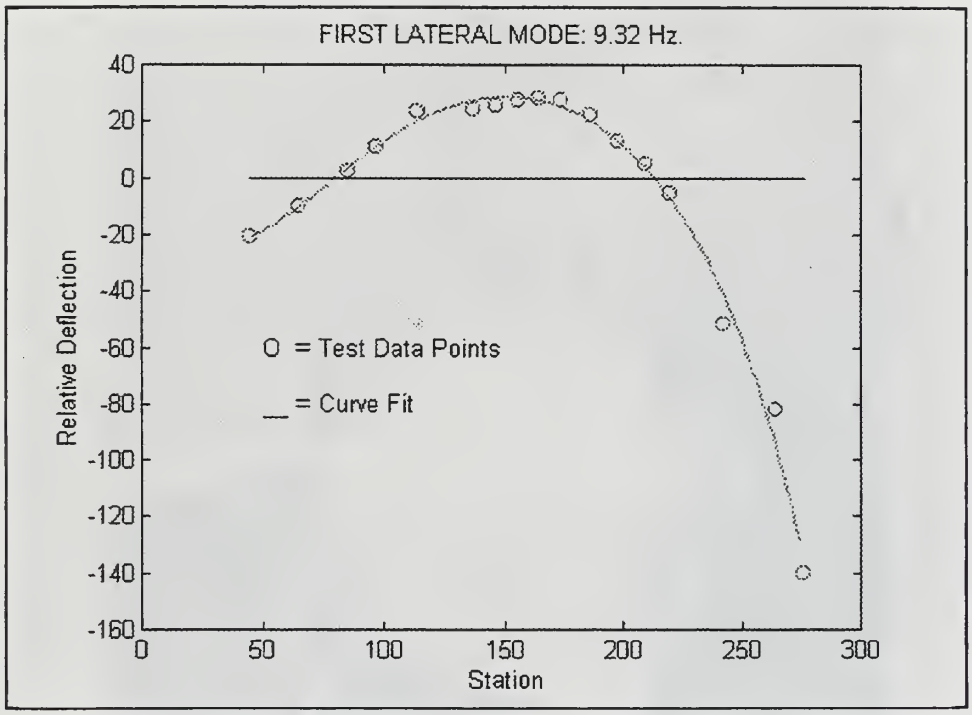

Figure 11. First Lateral Mode.

Figure 11 demonstrates the relatively high flexibility of the tail boom in relation to the fuselage as expected. Also the two nodes are located at stations 80 and 214. This can be verified by shaking the aircraft at a high power setting (greater than 20 lbs) and physically feeling little or no vibration near the nodes while simultaneously witnessing large deflections near the tail.

The second lateral mode was determined using a shaker input load of 20 lbs. A narrow band frequency sweep from 25 to 30 Hz was performed to isolate the modal characteristics. Nodes were located at stations 54, 136, and 287 as depicted in Figure 12.

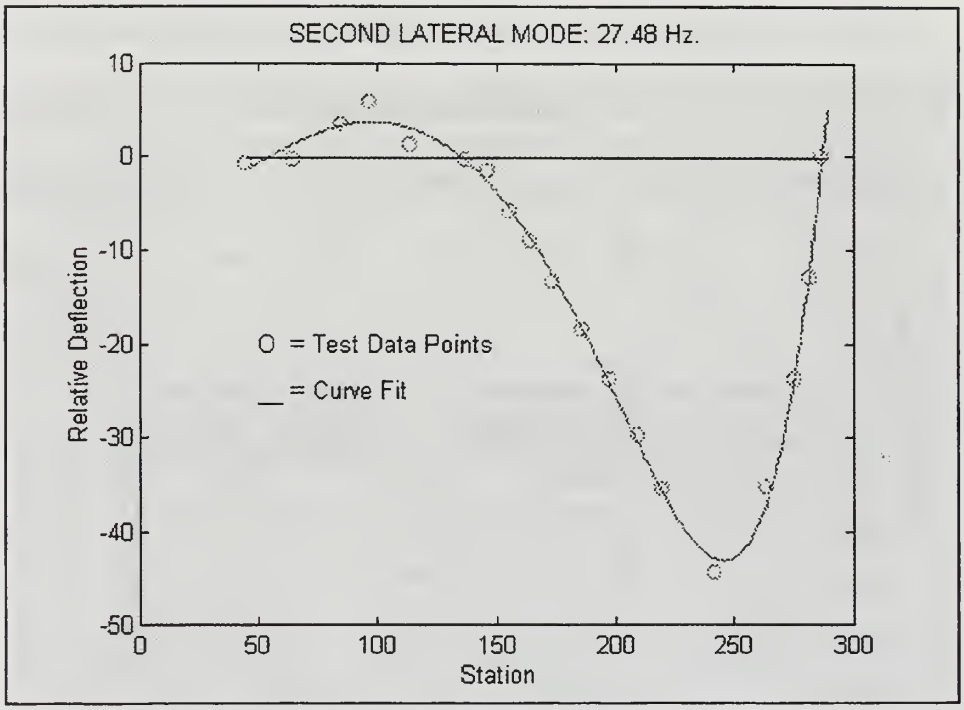

Figure 12. Second Lateral Mode.

4. First and Second Vertical Modes

The first and second vertical modes were obtained in a similar manner as the first and second lateral modes, however, the shaker was placed on the floor (see Figure 13) to excite the airframe vertically in an effort to better localize the vertical modes. Accelerometer measuring points matched those used in the first lateral mode sweep, although, the accelerometer was mounted such that its vertical axis was perpendicular to the floor and the longitudinal axis of the aircraft. A frequency sweep from 8 to 12 Hz.

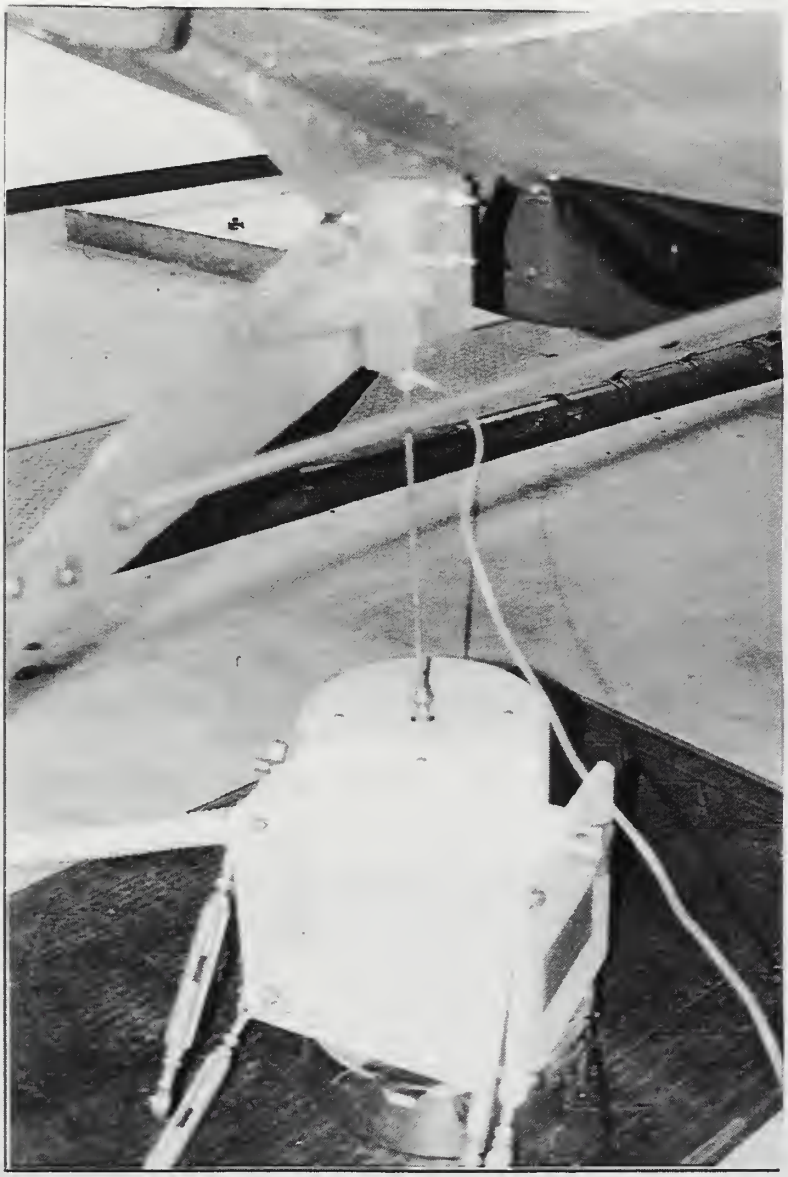

Figure 13. Vertical Excitation of Helicopter.

was used to isolate the first vertical modal response. Using the previously mentioned criteria to determine the natural frequency and the imaginary scale values at that frequency, Figure 14 was obtained. The nodes were located at stations 87 and 202.

What McDonnell Douglas had tentatively identified as the second vertical mode did not exhibit characteristics of a classical second mode as can be seen by Figure 15.

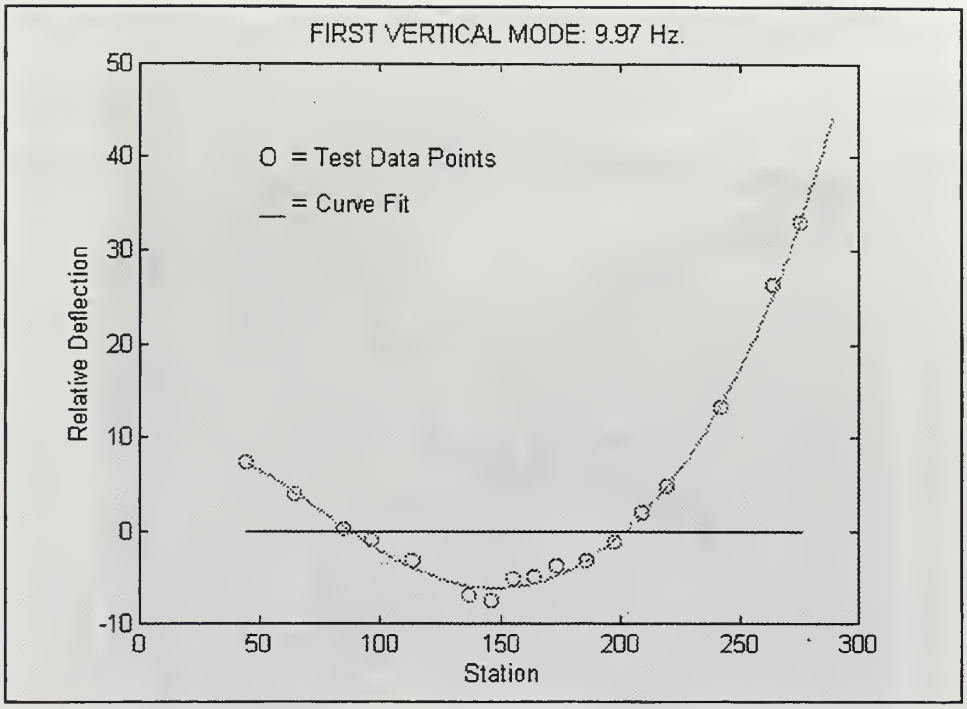

Figure 14. First Vertical Mode.

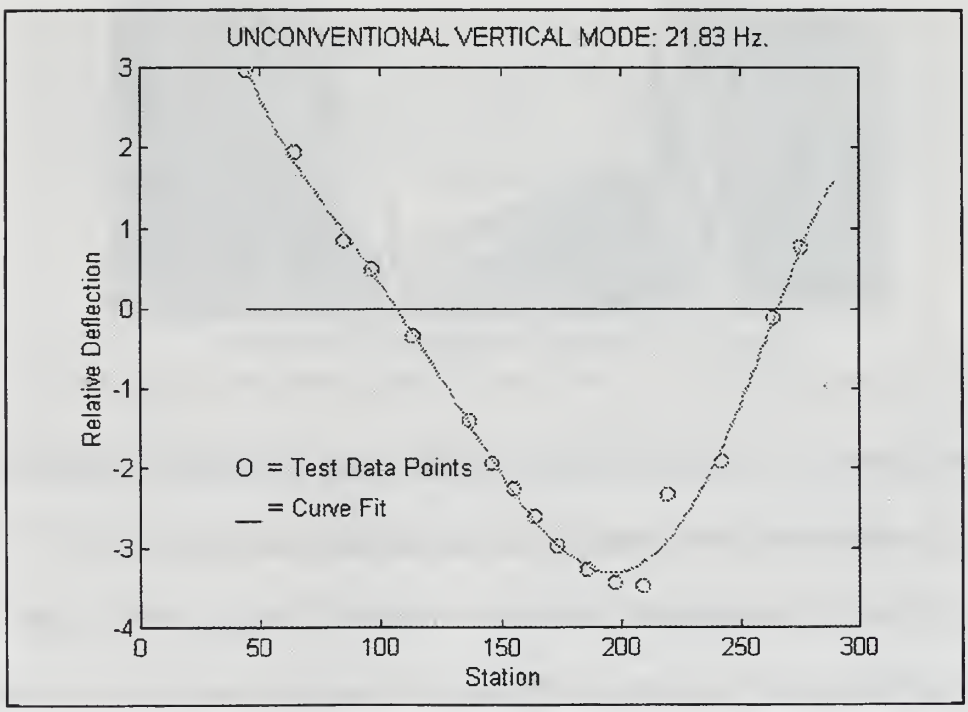

Figure 15. Unconventional "Second" Vertical Mode.

One would expect the modal curve to bend and form an additional node near the nose of the aircraft (station 44). To verify that the mode was vertical, the accelerometer was placed at the lateral measurement point at station 200 (where acceleration measurements were maximum), and while dwelling on the resonant frequency, the accelerometer was gradually moved toward the vertical measurement point. This revealed a maximum acceleration value in the vertical direction, thus suggesting a vertical mode.

Possible explanations for this apparent discrepancy include interference from a nearby mode, measurement error, or the possibility that the mode is actually a coupled lateral / vertical / torsion mode. It is important to recognize in studying vibrations of complex airframe structures that there is a tendency for engineers to assign classical titles based upon conventional beam response. At times, as in this case, such titles can be misleading.

5. First Torsional Mode

The first torsional mode was observed at 15.01 Hz. The mode was most obvious in the empennage section where large acceleration measurements were present due to the moment arms of the angled stabilizer and the vertical stabilizer. The mode did not rotate directly about the longitudinal axis of the tailboom, as is evident in Figure 16. The fuselage was also tested for torsion, but only negligible rotations were present.

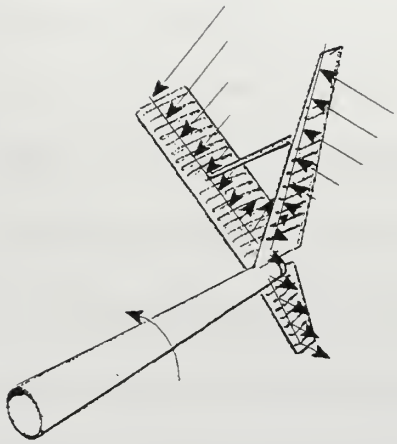

Figure 16. Motion Produced by First Torsional Mode.

6. Damping

Damping was measured using the *3-dB down point* (*half-power point*) method. Inman [Ref. 9] explains that for systems with light enough damping , such that the peak of the transfer function at resonance is well defined, the modal damping ratio is related to the frequencies corresponding to the two points of the magnitude plot by

$$\zeta = \frac{\omega_b - \omega_a}{2\omega_d}.$$

Here ω_d is the damped natural frequency at resonance and ω_a and ω_b are the frequencies corresponding to a magnitude that is 3 dB less than the peak (resonant) magnitude.

Damping values were calculated for those natural frequencies which were evaluated for mode shapes. The linearity of the damping ratio was also checked by comparing damping ratios at different force levels. Through the range limited by the

shaker, damping remained essentially constant. Damping values for different modes are shown in Table 6. The differing values are a function of the structural characteristics of the airframe.

Mode	Damping Ratio (ζ)
First Lateral	0.0184
Second Lateral	0.0222
First Vertical	0.0155
Second Vertical	0.0176
First Torsional	0.0150

Table 6. Damping Ratios Measured at Various Natural Frequencies.

Note that test values obtained for structural damping range from 1.5% to 2.22%. These values are consistent with the standard textbook value of airframe structure damping, which is 2.0%. Since 2.0% is considered a conservative number, the OH-6A damping values obtained from these tests would indicate that the airframe is somewhat less damped than a representative fixed wing aircraft.

IV. COMPARISON OF RESULTS

A. MCDONNELL DOUGLAS HELICOPTER COMPANY TESTING

In 1990 the McDonnell Douglas Helicopter Company (MDHC) prepared a report under U. S. Government Contract NAS1-17498 which addressed the study of finite element modeling of the OH-6A airframe [Ref. 6]. The report explained the development of a NASTRAN model which was used to calculate vibration characteristics of the helicopter airframe. The model was then verified by performing a correlation between calculated data and measured data obtained from a ground vibration test conducted in 1981. The correlation criteria involved a comparison of natural frequencies and the qualitative nature of mode shapes.

B. COMPARISON OF MDHC AND NPS RESULTS

The data contained in the NASA report served as a guideline for measurements taken during the NPS vibration tests. There were, however, key differences between the configurations of the NPS helicopter and the McDonnell Douglas aircraft, thus some disparity existed between test results and MDHC data. The fundamental difference among the aircraft was the distribution of weight. Table 7 provides a summary of the weight and center of gravity dissimilarities.

As a result of the differences described in Table 7, the natural frequencies of the NPS configuration are slightly higher than their MDHC counterparts. This phenomenon is inherently obvious due to the inverse relationship of frequency and weight. Table 8 contains a summary of mode comparisons between the MDHC and NPS data.

	NPS Configuration		MDHC Configuration	
Item Description	Weight (lbs)	Fuselage Station (in)	Weight (lbs)	Fuselage Station (in)
Ship as weighed	1311	105.1	1369	105.1
Crew (2) ballast	0		420	73.5
Fuel ballast	0		400	98.3
Additional Ballast	80	105.1	330	112.5
Total Weight / c.g. location	1391	105.1	2519	99.7

Table 7. Weight Dissimilarities Between NPS and MDHC Configurations

Mode	MDHC Test (Hz)	NPS Test (Hz)	% Difference
First Lateral	8.40	9.32	9.9
First Vertical	9.30	9.97	6.7
First Torsional	14.40	15.01	4.1
Aft Vertical	15.50	15.61	0.7
Second Vertical	20.70	21.83	5.2
Second Lateral	26.40	27.48	3.9

Table 8. Comparison of MDHC and NPS Mode Frequencies

V. CONCLUSIONS / RECOMMENDATIONS

A. CONCLUDING REMARKS

To date, the most significant obstacles facing the helicopter industry are vibration and noise reduction. The two are closely interrelated, yet their solutions remain perplexingly elusive. The key to solving these problems is a full comprehension of helicopter dynamics.

Two concepts are central to understanding helicopter dynamics. First, the main and tail rotors serve as the principal vibration source, and they act as a filter by transmitting mainly *1P* and *nP* vibrations into the fuselage. Second, large structural responses to main and tail rotor inputs indicate potential flight vibration problems.

Vibration measurement tests and analytic modeling are the two methods used to determine structural responses to dynamic inputs. This thesis develops measurement techniques which can be used to verify future analytic models of the OH-6A. The techniques can also be applied to other vibration tests.

The goals of the research were to establish the principal natural frequencies of the OH-6A airframe and, where feasible, to generate mode shapes. The testing portion of the thesis proved very successful in reaching the goals. Seven natural frequencies were detected and mode shapes for five of those natural frequencies were developed. Moreover, the experimental data closely correlated to figures supplied by the McDonnell Douglas Helicopter Company in previous tests.

B. RECOMMENDATIONS FOR FURTHER RESEARCH

1. Test Improvements

Although the testing performed for this thesis was successful, the procedure and equipment can still be improved. Recommendations for future testing include:

1. Upgrade the analyzer to include multi-input multi-output (MIMO) technology. For example, Zonic A&D's Workstation 7000 series high-speed parallel signal processors can support over 32 channels, thereby significantly decreasing test time and improving the accuracy of results. By negating the need to constantly move a single roving accelerometer for each modal analysis, test parameters remain more consistent. Reducing the time required for a modal survey allows for a more complete analysis of target data. An interesting capability of the Zonic A&D system is its ability to interface with I-DEAS software, enabling the user to more closely correlate test data and analytic model data.

2. Improve transducers (accelerometer and load cell) to alleviate the problem of non-axial motion pick-up. State-of-the-art accelerometers are available today which use laser and fiber-optic technologies to measure motion. These *vibrometers* operate by illuminating the vibrating structure with laser light and using Doppler frequencies and interference fringes to measure amplitudes of displacement and velocity [Ref. 7].

3. Consideration should be given to more closely matching actual flight weight characteristics (i.e., the McDonnell Douglas configuration), specifically fuel and crew criteria. Safety precautions precluded the presence of fuel in the fuel tanks during testing. Also, retaining the flight worthiness of the helicopter remained a central issue. At the time of testing, a final decision was not yet made in choosing which helicopter would remain operational and which would serve as an experimental testbed. As a result, placing an inert substance in the fuel system was not a viable alternative. Once the final decision is made concerning the assignment of the two helicopters, the use of an inert substance in the fuel tanks will be feasible. Additional compensation for the weight of the crew would then be more sensible.

4. Designate a laboratory for helicopter dynamic testing and analysis. Testing for this thesis was conducted in room 101 Halligan Hall, however, plans are in effect to convert this room to a machine shop. Requirements of a new laboratory include:

a. space large enough to accommodate the OH-6A helicopter, and
b. ability to secure all equipment under lock and key.

A current area under consideration is located in front of the P2-V wing, although this space would require alterations to enhance security.

5. Develop an analytic model for comparison to test results. Establishing expertise in computer dynamic analysis modeling will greatly enhance the capabilities and prestige of the NPS helicopter dynamics program. The OH-6A serves as an excellent building block in achieving such expertise. The airframe is relatively uncomplicated and should be easy to model using software such as I-DEAS or NASTRAN / PATRAN. Recently, the McDonnell Douglas Helicopter Company provided NPS with a NASTRAN model of the MD 500, which closely resembles the OH-6A. This model can be adjusted to match the testing conditions for this thesis, and analytic data can be checked against test data from this thesis. Once completed, the model would serve as an excellent teaching tool due to its relative simplicity.

APPENDIX A: FREQUENCY RESPONSE FUNCTION DATA CONVERSION

```
% Program:  Data Conversion
% Program received from LCDR James Speer
% The purpose of this program is to convert DSA frequency
% response raw data (a set of real and imaginary points) to
% data that can be plotted in MATLAB on a linear or dB scale.
% To use the program, the data file must first be loaded as
% follows:
%       load(fname);
%       a=fname(:,2);
%

k=1;
j=2;
for i=1:1:801
  R(i)=a(k);
  k=k+2;
end
for i=1:1:801
 I(i)=a(j);
 j=j+2;
end
for i=1:1:801
    m(i)=(R(i)^2+I(i)^2)^0.5;
end
step=40/801;
f=[5:step:45-step];
for i=1:1:801
  d(i)=20*log10(m(i));
end
subplot(211),plot(f,d)
subplot(211),xlabel('Frequency (Hz.)')
subplot(211),ylabel('Frequency Response (dB)')
subplot(212),plot(f,m)
subplot(212),xlabel('Frequency (Hz.)')
subplot(212),ylabel('Frequency Response (Linear)')
```

APPENDIX B: FRF PLOTS

Appendix B contains sample plots identifying the principal modes from 0 to 45 Hz. The frequency span was divided into three smaller spans to better locate the natural frequencies. Sine sweeps were performed in each interval, and plots were obtained depicting real, imaginary, phase, and magnitude values.

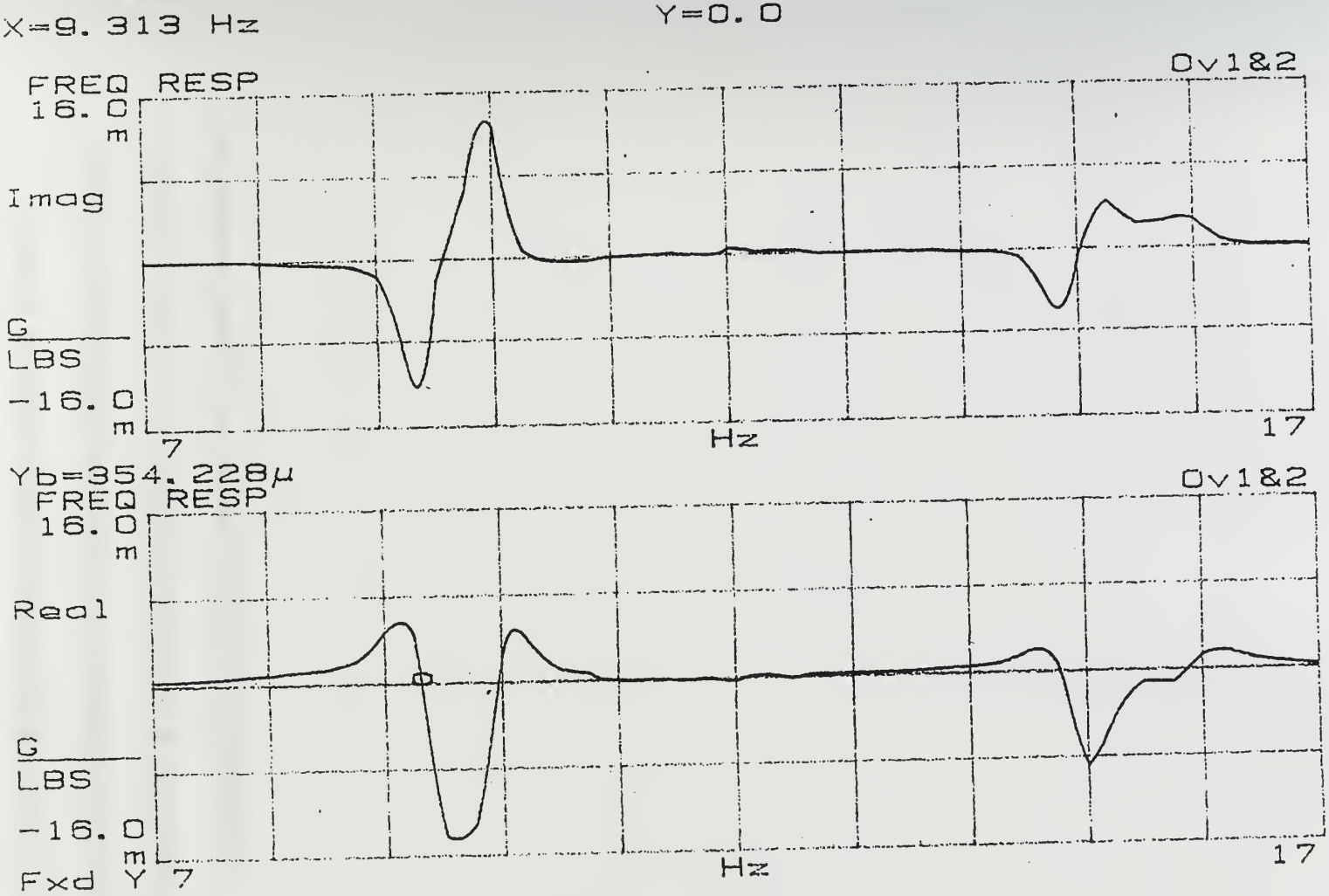
X=9.313 Hz
Y=0.0
FREQ RESP
0v1&2
16.0
m
Imag
G
LBS
-16.0
m
7
Hz
17
Yb=354.228μ
FREQ RESP
0v1&2
16.0
m
Real
G
LBS
-16.0
m
Fxd Y 7
Hz
17

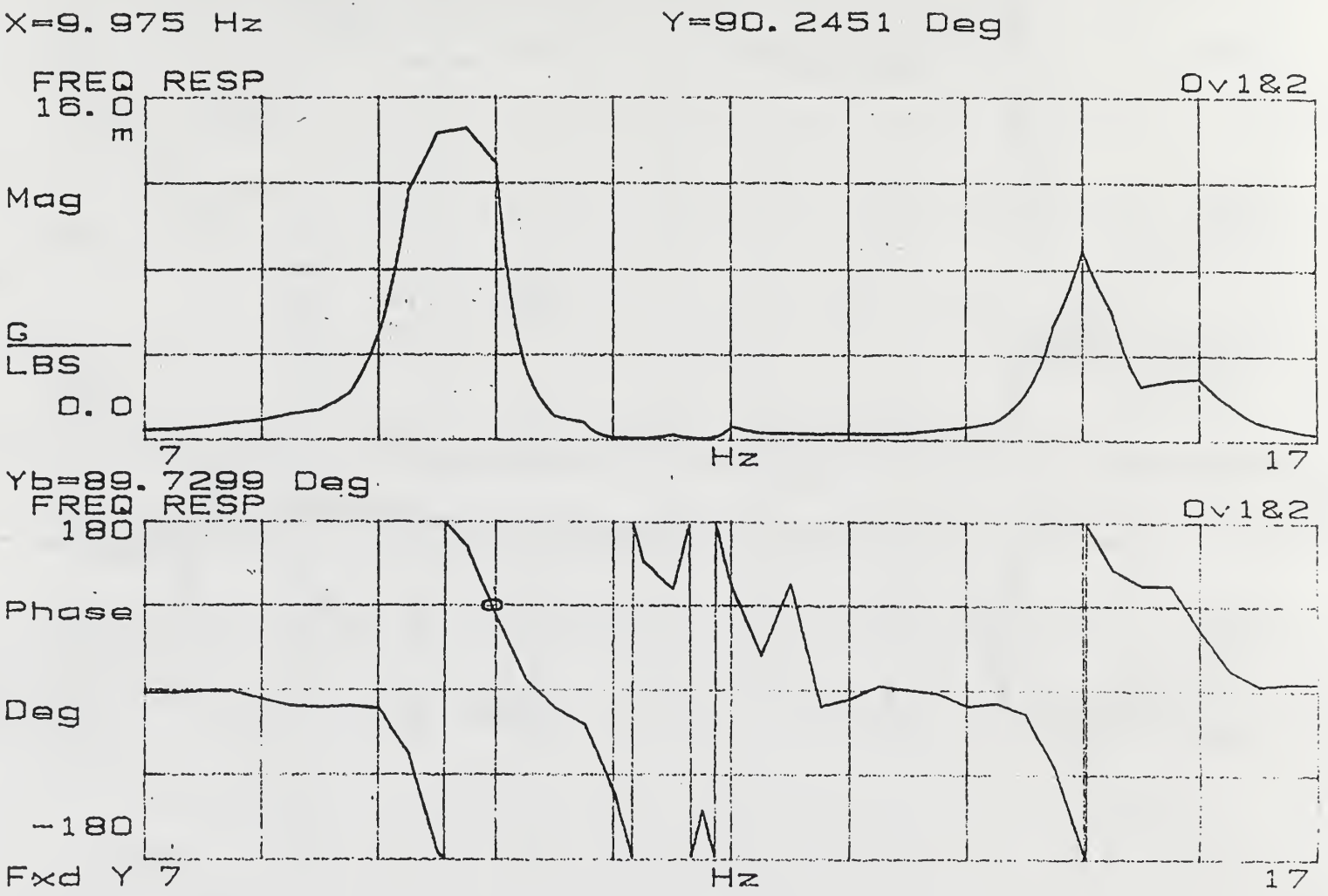
X=9.975 Hz
Y=90.2451 Deg
FREQ RESP
Ov1&2
16.0
m
Mag
G
LBS
0.0
7
Hz
17
Yb=89.7299 Deg
FREQ RESP
Ov1&2
180
Phase
Deg
-180
Fxd Y 7
Hz
17

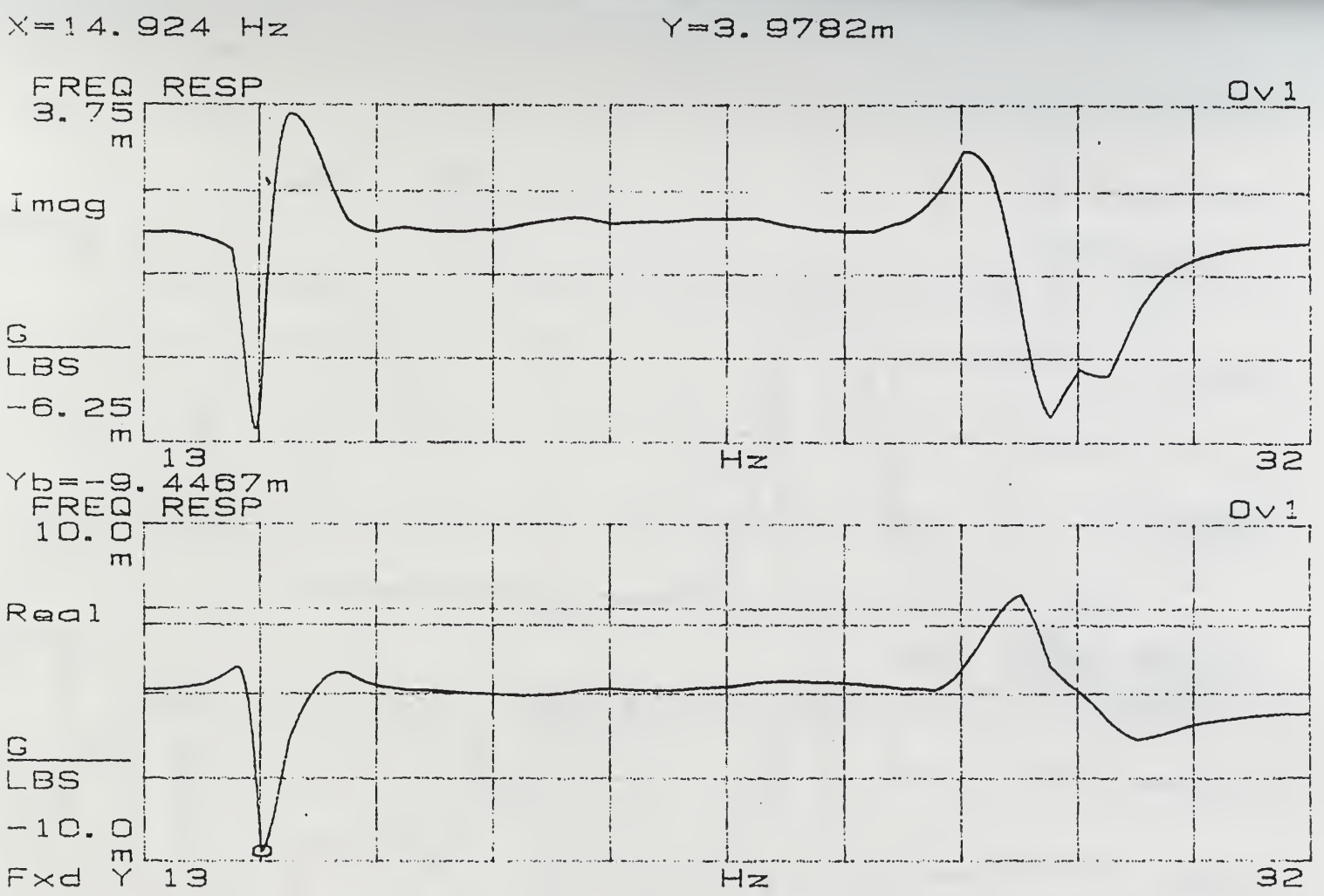
X=14.924 Hz
Y=3.9782m
FREQ RESP
Ov1
3.75
m
Imag
G
LBS
-6.25
m
13
Hz
32
Yb=-9.4467m
FREQ RESP
Ov1
10.0
m
Real
G
LBS
-10.0
m
Fxd Y
13
Hz
32

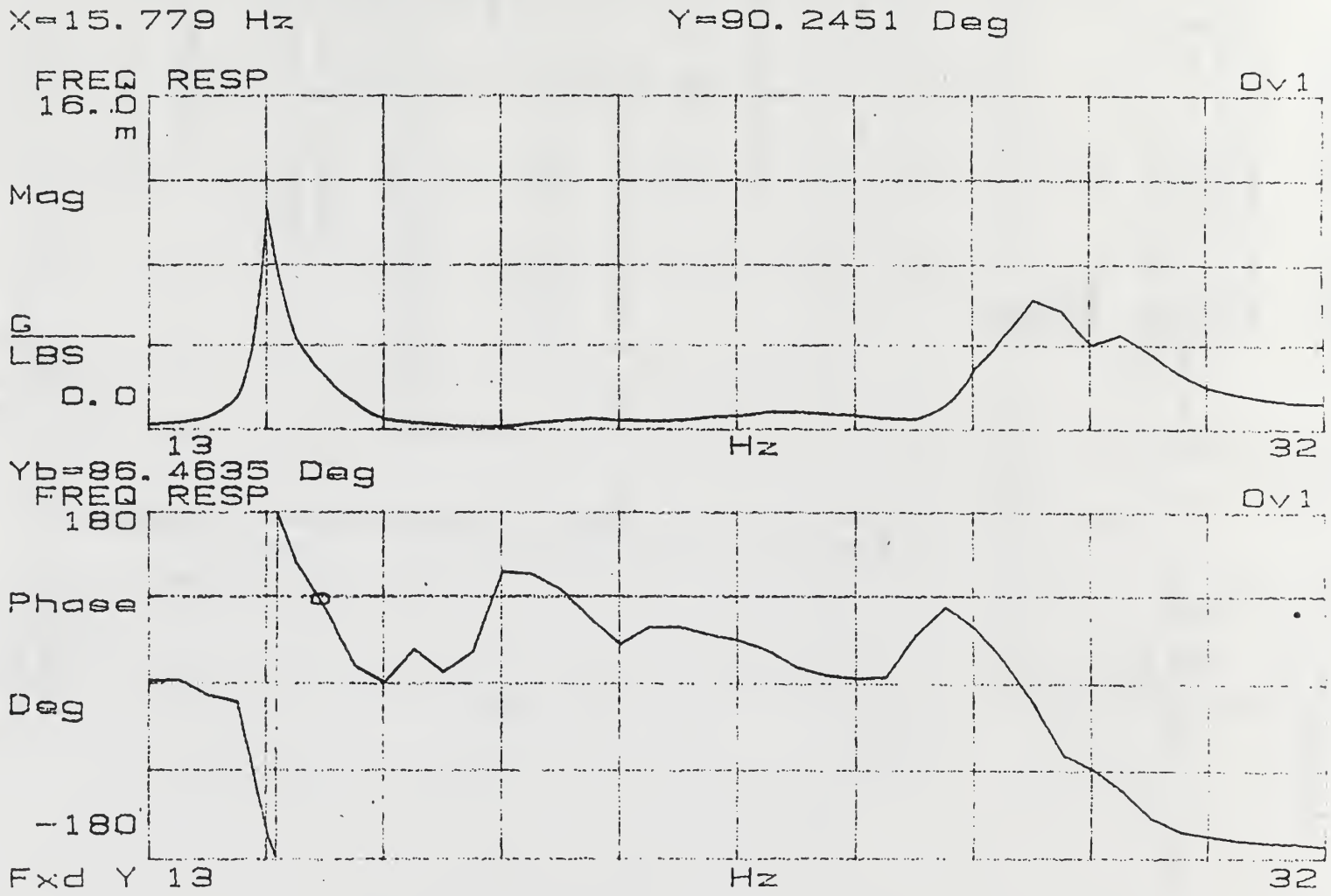
X=15.779 Hz
Y=90.2451 Deg
FREQ RESP
Ov1
16.0
m
Mag
G
LBS
0.0
13
Hz
32
Yb=86.4635 Deg
FREQ RESP
Ov1
180
Phase
Deg
-180
Fxd Y 13
Hz
32

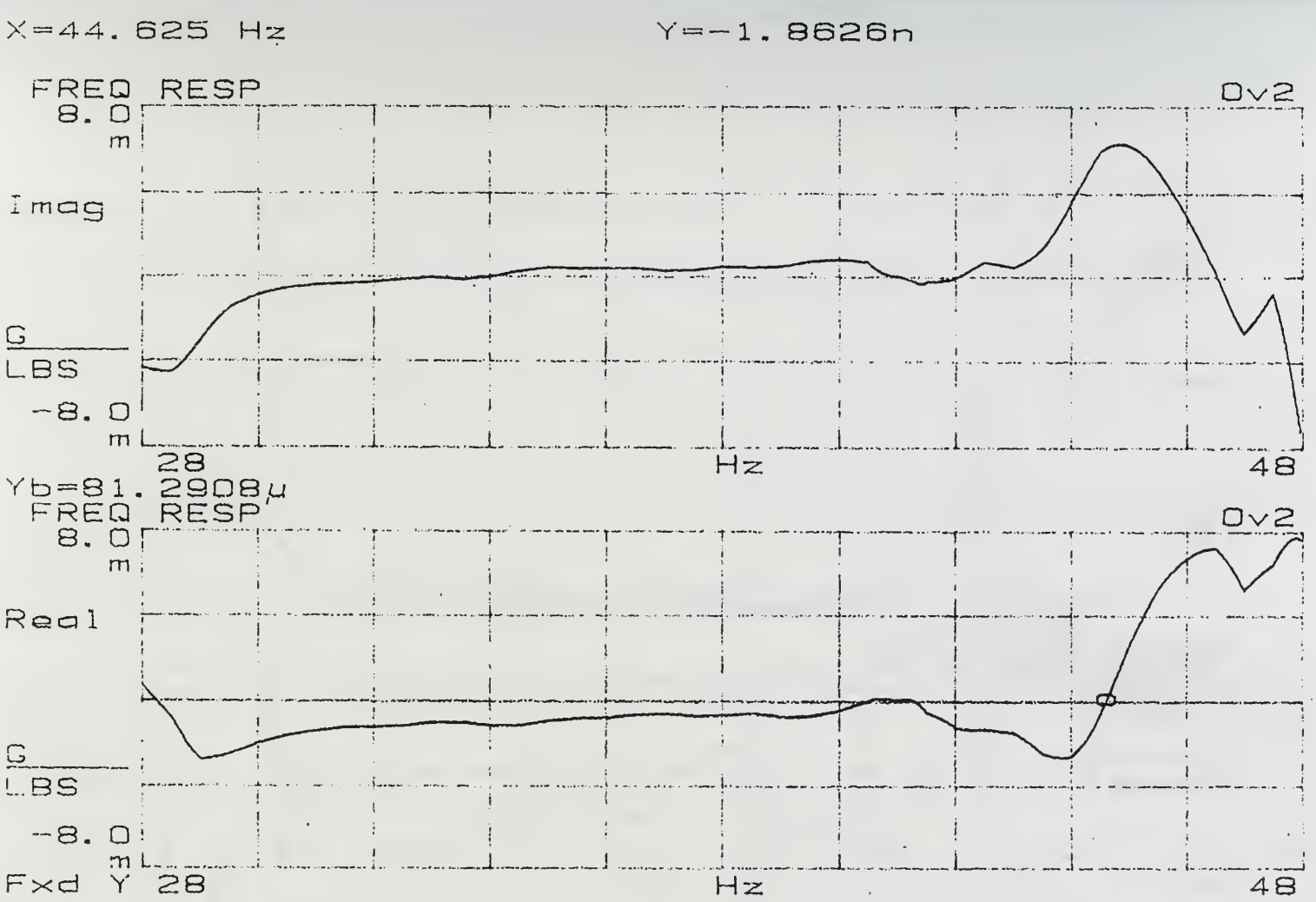
X=44.625 Hz
Y=-1.8626n
FREQ RESP
Ov2
8.0
m
Imag
G
LBS
-8.0
m
28
Hz
48
Yb=81.2908μ
FREQ RESP
Ov2
8.0
m
Real
G
LBS
-8.0
m
Fxd Y 28
Hz
48

APPENDIX C: MODE SHAPE PLOTTING PROGRAM

```
% Mode Shape Plotting Program
% Program written by John Harris
% The following program plots mode shapes with manually entered data.  Curves
% are fit to the points to show trends.

clear

x=[44.65 64.36 84.79 96.42 113.85 137.50 146.62 155.75 164.67 ...
   174 185.89 197.78 209.78 219.96 242.14 264.32 275.57]';

y_l1=[-20.839 -9.8965 2.0534 11.1376 23.564 24.2915 25.7875 27.7057 ...
   28.4033 27.6185 22.117 12.69 5.1226 -5.58 -51.8801 -82.343 -140.19]';
y_l2=[-.616 -.343 3.42016 5.8998 1.28174 -.217 -1.4801 -5.891 -9.0354 ...
  -13.411 -18.55 -23.913 -29.82 -35.586 -44.425 -35.444 -23.956 -12.932 .132]';
%
% First Lateral Mode
%
p_l1=polyfit(x,y_l1,5);

for i=1:1:230 %adjust this number to extend to tip of tail
  xm_l1(i)=44+i;
  mode_l1(i)=polyval(p_l1,xm_l1(i));
end
whitebg
figure
plot(x,y_l1,'o',xm_l1,mode_l1,x,zeros(17,1))
title('FIRST LATERAL MODE: 9.32 Hz.')
xlabel('Station')
ylabel('Relative Deflection')
text(50,-60,'O  = Test Data Points')
text(50,-80,'__ = Curve Fit')

node_l1=roots(p_l1)
%
% Second Lateral Mode
%
x_l2=[44.65 64.36 84.79 96.42 113.85 137.50 146.62 155.75 164.67 ...
       174 185.89 197.78 209.78 219.96 242.14 264.32 275.57 282 287]';
p_l2=polyfit(x_l2,y_l2,6);

for i=1:1:245 %adjust this number to extend to tip of tail
```

```
 xm_l2(i)=44+i;
 mode_l2(i)=polyval(p_l2,xm_l2(i));
end

figure
plot(xm_l2,mode_l2,x_l2,y_l2,'o',xm_l2,zeros(245,1))
title('SECOND LATERAL MODE: 27.48 Hz.')
xlabel('Station')
ylabel('Relative Deflection')
text(50,-20,'O  = Test Data Points')
text(50,-25,'__ = Curve Fit')

node_l2=roots(p_l2)
%
% First Vertical Mode.
%
x_v1=[44.65 64.36 84.79 96.42 113.85 137.50 146.62 155.75 164.67 ...
       174 185.89 197.78 209.78 219.96 242.14 264.32 275.57]';
y_v1=[7.2153 3.8583 .232e-3 -1.0109 -3.3242 -7.0845 ...
    -7.6948 -5.1967 -5.0398 -3.874 -3.3242 -1.2556 1.82016 ...
     4.69972 13.2098 26.2452 32.9155]';

p_v1=polyfit(x_v1,y_v1,5);

for i=1:1:245 %adjust this number to extend to tip of tail
 xm_v1(i)=44+i;
 mode_v1(i)=polyval(p_v1,xm_v1(i));
end

figure
plot(x_v1,y_v1,'o',xm_v1,mode_v1,x_v1,zeros(17,1))
title('FIRST VERTICAL MODE: 9.97 Hz.')
xlabel('Station')
ylabel('Relative Deflection')
text(50,40,'O  = Test Data Points')
text(50,35,'__ = Curve Fit')

node_v1=roots(p_v1)
%
% Second Vertical Mode
%
x_v2=[44.65 64.36 84.79 96.42 113.85 137.50 146.62 155.75 164.67 ...
     174 185.89 197.78 209.78 219.96 242.14 264.32 275.57]';
```

```
y_v2=[2.9556 1.9342 .832 .490 -.347 -1.4015 -1.9482 -2.268 -2.6158 ...
    -2.9733 -3.2916 -3.455 -3.4877 -2.3296 -1.9118 -.110 .769]';

p_v2=polyfit(x_v2,y_v2,5);

for i=1:1:245 %adjust this number to extend to tip of tail
  xm_v2(i)=44+i;
  mode_v2(i)=polyval(p_v2,xm_v2(i));
end

figure
plot(x_v2,y_v2,'o',xm_v2,mode_v2,x_v2,zeros(17,1))
title('SECOND VERTICAL MODE: 21.83 Hz.')
xlabel('Station')
ylabel('Relative Deflection')
text(40,-2,'O  = Test Data Points')
text(40,-2.5,'__ = Curve Fit')

node_v2=roots(p_v2)

%
% First Torsional Mode
%

ht_x=[7.25 22.75 38 50.75 65.75]';
vt_x=[-28.5 -20.5 -12.5 -4.5 7.5 20.5 33.5 51.5]';
% vtbot_x=[1 9 17 25]';

ht_y=[13.079 -33.243 -91.553 -168.94 -235.75]';
vt_y=[103.379 80.544 60.2861 37.886 12.0763 -24.937 -75.204 -151.72]';
% vtbot_y=[37.8856 60.2861 80.544 103.379]';

p_ht=polyfit(ht_x,ht_y,2);
p_vt=polyfit(vt_x,vt_y,5);
% p_vtbot=polyfit(vtbot_x,vtbot_y,3);


for i=1:1:66 %adjust this number to extend to tip of horiz stab
  xm_ht(i)=i;
  mode_ht(i)=polyval(p_ht,xm_ht(i));
end

for i=1:1:82;
```

```
 xm_vt(i)=i-30;
 mode_vt(i)=polyval(p_vt,xm_vt(i));
end

figure
plot(ht_x,ht_y,'o',xm_ht,mode_ht,vt_x,vt_y,'o', ...
    xm_vt,mode_vt,vt_x,zeros(8,1))
title('FIRST TORSIONAL MODE: 15.01 Hz.')
xlabel('Distance From Tailboom')
ylabel('Relative Deflection')
%text(40,-2,'O  = Test Data Points')
%text(40,-2.5,'__ = Curve Fit')
```

LIST OF REFERENCES

1. Wood, E. R. , "An Introduction to Helicopter Dynamics," *An Introduction to Helicopter Engineering*, Hughes Helicopters, Inc. and Graduate Aeronautical Laboratories California Institute of Technology, 1984.

2. Thomson, W.T., *Mechanical Vibrations*, Prentice-Hall Inc., New York, N.Y., 1948.

3. Wood, E. R., Powers, R. W., Cline, J. H., and Hammond, C. E., "On Developing and Flight Testing a Higher Harmonic Control System," *Journal of the American Helicopter Society*, Vol. 30, No. 1, January 1985.

4. Gerstenberger, Walter, and Wood, E. R., "Analysis of Helicopter Aeroelastic Characteristics in High-Speed Flight," *American Institute of Aeronautics and Astronautics Journal*, Vol. 1, No. 10, October 1963.

5. Johnson, Wayne, *Helicopter Theory*, Princeton University Press, Princeton, New Jersey, 1980.

6. *Aviation Unit and Intermediate Maintenance Manual: Helicopter, Observation OH-6A*, Headquarters, Deptartment of the Army, Washington, D.C., 1981.

7. Ferg, Douglas and Toosi, Mostafa, *NASA Contractor Report 187449: Finite Element Modeling of the Higher Harmonic Controlled OH-6A Helicopter Airframe*, National Aeronautics and Space Administration, Hampton, Virginia, 1990.

8. Bielawa, Richard L., *Rotary Wing structural Dynamics and Aeroelasticity*, American Institute of Aeronautics and Astronautics, Inc., Washington, D.C., 1992.

9. Inman, Daniel J., *Engineering Vibration*, Prentice-Hall Inc., Englewood Cliffs, New Jersey, 1994.

INITIAL DISTRIBUTION LIST

No. Copies

1. Defense Technical Information Center. 2
   8725 John J. Kingman Rd., STE 0944
   Ft. Belvoir, VA 22060-6218

2. Dudley Knox Library 2
   Naval Postgraduate School
   411 Dyer Rd.
   Monterey, Ca 93943-5100

3. Department of Aeronautics and Astronautics, Code AA 2
   Naval Postgraduate School
   Monterey, Ca 93943-5000

4. Professor E. Roberts Wood, Code AA/Wd 4
   Department of Aeronautics and Astronautics
   Naval Postgraduate School
   Monterey, Ca 93943-5000

5. Professor Joshua H. Gordis, Code ME/Go 1
   Department of Mechanical Engineering
   Naval Postgraduate School
   Monterey, Ca 93943-5000

6. Professor Donald A. Danielson, Code MA/Dd 1
   Department of Mathematics
   Naval Post Graduate School
   Monterey, Ca 93943-5000

7. MAJ Vince Tobin, Code 31 1
   Department of Aeronautics and Astronautics
   Naval Postgraduate School
   Monterey, Ca 93943-5000

8. LT John Harris, Code 31 1
   238 Carlyle Lake Dr.
   Creve Coeur, MO 63141

9. Robert L.Tomaine 1
   436 Mason ridge Drive
   St. Charles, MO 63304

10. Dr. Sam T. Crews 1
6904 Washington
University City, MO 63130

11. Mostafa Toosi 1
8126 E. Quarterhorse
Scottsdale, Az 85258

12. Raymond G. Kvaternik 1
103 Pocomoke Run
Yorkstown, VA 23693

13. Dr. Friedrich Karl Straub 1
1760 E. Halifax St.
Mesa, AZ 85203

14. John C. McKeown. 1
315 Braehead Dr.
Fredericksburg, VA 22401

15. Robert H. Blackwell, Jr. 1
103 Old Zoar Rd.
Monroe CT 06468

16. Dr. D. J. Taylor 1
608 Thicket Lane
Lake St. Louis, MO 63367

17. LTG(Ret) William H. Forster 1
10245 Fairfax Dr.
Ft. Belvoir, VA 22060-2123

18. General James Snider 1
Program Manager, Comanche
4300 Goodfellow Blvd.
St. Louis, MO 63120-1798